

Calculation of Moon Phases and 24 Solar Terms

Yuk Tung Liu (廖育棟)

First draft: 2018-10-24, Last major revision: 2021-06-12

Chinese Versions: 傳統中文 簡體中文

This document explains the method used to compute the times of the moon phases and 24 solar terms. These times are important in the calculation of the Chinese calendar. See this page for an introduction to the 24 solar terms, and this page for an introduction to the Chinese calendar calculation.

Computation of accurate times of moon phases and 24 solar terms is complicated, but today all the necessary resources are freely available. Anyone familiar with numerical computation and computer programming can follow the procedure outlined in this document to do the computation.

Before stating the procedure, it is useful to have a basic understanding of the basic concepts behind the computation. I assume that readers are already familiar with the important astronomy concepts mentioned on this page. In Section 1, I briefly introduce the barycentric dynamical time (TDB) used in modern ephemerides, and its connection to terrestrial time (TT) and international atomic time (TAI). Readers who are not familiar with general relativity do not have to pay much attention to the formulas there. Section 2 introduces the various coordinate systems used in modern astronomy. Section 3 lists the formulas for computing the IAU 2006/2000A precession and nutation matrices.

One important component in the computation of accurate times of moon phases and 24 solar terms is an accurate ephemeris of the Sun and Moon. I use the ephemerides developed by the Jet Propulsion Laboratory (JPL) for the computation. Section 4 introduces the JPL ephemerides and describes how they can be downloaded and used to compute the positions and velocities of solar system objects. One of the main goals of the JPL ephemerides is for spacecraft navigation. Positions and velocities of the solar system objects are given in the international celestial reference system (ICRS). Hence, these data need to be transformed to the ecliptic coordinate system suitable for the computation of the moon phases and 24 solar terms. Section 5 describes the light-time correction and aberration of light. Section 6 provides a step-by-step procedure for computing the apparent geocentric longitude of the Sun and Moon from the data computed from the JPL ephemerides. Section 7 describes the numerical method for computing the TDB times of the moon phases and 24 solar terms from the apparent geocentric longitudes of the Sun and Moon. Finally, Section 8 describes the conversion of times between TDB and UTC+8 necessary for calendar calculation. For a more detailed and comprehensive introduction to the concepts mentioned in this document, I recommend the book *Explanatory Supplement to the Astronomical Almanac* by [Urban & Seidelmann 2013].

1 Ephemeris Time and Barycentric Dynamical Time

From the 17th century to the late 19th century, planetary ephemerides were calculated using time scales based on Earth’s rotation. It was assumed that Earth’s rotation was uniform. As the precision of astronomical measurements increased, it became clear that Earth’s rotation is not uniform. Ephemeris time (ET) was introduced to ensure a uniform time for ephemeris calculations. It was defined by the orbital motion of the Earth around the Sun instead of Earth’s spin motion. However, a more precise definition of times is required when general relativistic effects need to be included in ephemeris calculations.

In general relativity, the passage of time measured by an observer depends on the spacetime trajectory of the observer.¹ To calculate the motion of objects in the solar system, the most convenient time is a coordinate time, which does not depend on the motion of any object but is defined through the spacetime metric. In the *Barycentric Celestial Reference System* (BCRS), the spacetime coordinates are (t, x^i) ($i = 1, 2, 3$). Here the time coordinate t is called the *barycentric coordinate time* (TCB). The spacetime metric for the solar system can be written as [see Eq. (2.38) in [Urban & Seidelmann 2013]]

$$ds^2 = - \left(1 - \frac{2w}{c^2} + \frac{2w^2}{c^4} \right) d(ct)^2 - \frac{4w_i}{c^3} d(ct) dx^i + \delta_{ij} \left[1 + \frac{2w}{c^2} + O(c^{-4}) \right] dx^i dx^j, \quad (1)$$

where sum over repeated indices is implied. The scalar potential w reduces to the Newtonian gravitational potential $-\Phi$ in the Newtonian limit, where

$$\Phi(t, \mathbf{x}) = -G \int d^3x' \frac{\rho(t, \mathbf{x}')}{|\mathbf{x} - \mathbf{x}'|} \quad (2)$$

and ρ is the mass density. The vector potential w_i satisfies the Poisson equations with the source terms proportional to the momentum density.

TCB can be regarded as the proper time measured by an observer far away from the solar system and is stationary with respect to the solar system barycenter. The equations of motion for solar system objects can be derived in the post-Newtonian framework. The result is a system of coupled differential equations and can be integrated numerically. In this framework, TCB is the natural choice of time parameter for planetary ephemerides. However, since most measurements are carried out on Earth, it is also useful to set up a coordinate system with origin at the Earth’s center of mass. In the *geocentric celestial reference system* (GCRS), the spacetime coordinates are (T, X^i) , where the time parameter T is called the *geocentric coordinate time* (TCG). GCRS is comoving with Earth’s center of mass in the solar system, and its spatial coordinates X^i are chosen to be kinematically non-rotating with respect to the barycentric coordinates x^i . The coordinate time TCG is chosen so that the spacetime metric has a form similar to equation (1). Since GCRS is comoving with the Earth, it is inside the potential well of the solar system. As a result, TCG

¹Perhaps the best example to illustrate this effect is the Global Positioning System (GPS). The GPS navigation relies on comparing the times of emission and reception of radio waves from GPS satellites to the user. To achieve a navigation accuracy of 15 meters, time throughout the GPS system must be known to an accuracy of 50 nanoseconds, which simply corresponds to the time required for light to travel 15 meters. However, the GPS satellites are moving at 14,000 km/hr at an altitude of about 20,000 km from the ground. The combined effect of special and general relativistic time dilation results in the satellite clocks advancing faster than a clock on the ground by about 38.3 microseconds per day, or 26.6 nanoseconds per minute. If this effect is not taken into account, GPS would fail in its navigational functions within 2 minutes. See Clifford Will’s article “Einstein’s Relativity and Everyday Life” for a more detailed description.

elapses *slower* than TCB because of the combined effect of gravitational time dilation and special relativistic time dilation. The relation between TCB and TCG is given by [equation (3.25) in [Urban & Seidelmann 2013]]

$$\text{TCB} - \text{TCG} = c^{-2} \left[\int_{t_0}^t \left(\frac{v_e^2}{2} - \Phi_{\text{ext}}(\mathbf{x}_e) \right) dt + \mathbf{v}_e \cdot (\mathbf{x} - \mathbf{x}_e) \right] + O(c^{-4}), \quad (3)$$

where \mathbf{x}_e and \mathbf{v}_e are the barycentric position and velocity of the Earth's center of mass, and \mathbf{x} is the barycentric position of the observer. The external potential Φ_{ext} is the Newtonian gravitational potential of all solar system bodies apart from the Earth. The constant time t_0 is chosen so that $\text{TCB}=\text{TCG}=\text{ET}$ at the epoch 1977 January 1, 0h TAI.

Since the definition of TCG involves only external gravity, TCG's rate is faster than TAI's because of the relativistic time dilation caused by Earth's gravity and spin. The *terrestrial time* (TT), formerly called the terrestrial dynamical time (TDT), is defined so that its rate is the same as the rate of TAI. The rate of TT is slower than TCG by $-\Phi_{\text{eff}}/c^2$ on the geoid (Earth surface at mean sea level), where $\Phi_{\text{eff}} = \Phi_E - v_{\text{rot}}^2/2$ is the sum of Earth's Newtonian gravitational potential and the centrifugal potential. Here v_{rot} is the speed of Earth's spin at the observer's location. The value of Φ_{eff} is constant on the geoid because the geoid is defined to be an equipotential surface of Φ_{eff} . Thus, $d\text{TT}/d\text{TCG} = 1 - L_G$ and L_G is determined by measurements to be $L_G = 6.969290134 \times 10^{-10}$. Therefore, TT and TCG are related by a linear relationship [equation (3.27) in [Urban & Seidelmann 2013]]:

$$\text{TT} = \text{TCG} - L_G(\text{JD}_{\text{TCG}} - 2443144.5003725) \cdot 86400 \text{ s}, \quad (4)$$

where JD_{TCG} is TCG expressed as a Julian date (JD). The constant 2443144.5003725 is chosen so that $\text{TT}=\text{TCG}=\text{ET}$ at the epoch 1977 January 1 0h TAI ($\text{JD} = 2443144.5003725$). Since the rate of TT is the same as that of TAI, the two times are related by a constant offset:

$$\text{TT} = \text{TAI} + 32.184 \text{ s}. \quad (5)$$

The offset arises from the requirement that TT match ET at the chosen epoch.

TCB is a convenient time for planetary ephemerides, whereas TT can be measured directly by atomic clocks on Earth. The two times are related by equations (3) and (4) and must be computed by numerical integration together with the planetary positions. TT is therefore not convenient for planetary ephemerides. The *barycentric dynamical time* (TDB) is introduced to approximate TT. It is defined to be a linear function of TCB and is set as close to TT as possible. Since the rates of TT and TCB are different and are changing with time, TT cannot be written as a linear function of TCB. The best we can do is to set the rate of TDB the same as the rate of TT averaged over a certain time period, so that there is no long-term secular drift between TT and TDB over that time period. The resulting deviation between TDB and TT has components of periodic variation caused by the eccentricity of Earth's orbit and the gravitational fields of the Moon and planets. TDB is now defined by the IAU 2006 resolution 3 as

$$\text{TDB} = \text{TCB} - L_B(\text{JD}_{\text{TCB}} - 2443144.5003725) \cdot 86400 \text{ s} - 6.55 \times 10^{-5} \text{ s}, \quad (6)$$

where $L_B = 1.550519768 \times 10^{-8}$ and JD_{TCB} is TCB expressed as a Julian date (JD). The value of L_B can be regarded as $1 - d\text{TT}/dt$ averaged over a certain time period.

TDB is a successor of ET as the time standard used by modern high-precision ephemerides. The relationship between TT and TDB can be written as (Figure 3.2 in [Urban & Seidelmann 2013])

$$\text{TDB} = \text{TT} + 0.001658 \text{ s} \sin(g + 0.0167 \sin g)$$

$$\begin{aligned}
& + \text{lunar and planetary terms of order } 10^{-5} \text{ s} \\
& + \text{daily terms of order } 10^{-6} \text{ s},
\end{aligned} \tag{7}$$

where g is the mean anomaly of Earth in its orbit (and hence $g + 0.0167 \sin g$ is the approximate value of the eccentric anomaly since 0.0167 is Earth’s orbital eccentricity). A more detailed expression is given by equation (2.6) in [Kaplan 2005] and equation (3) in [Park et al 2021]. The difference between TDB and TT remains under 2 ms for several millennia around the present epoch. Thus, I treat them as the same for the calendar calculation.

2 Celestial Coordinate Systems

2.1 International Celestial Reference System (ICRS)

As mentioned in Section 1, the solar system metric can be written in the Barycentric Celestial Reference System (BCRS). The origin of the BCRS spatial coordinates is at the solar system barycenter, i.e. the center of mass of the solar system. However, BCRS is a dynamical concept. The statement of “we use BCRS” in general relativity is equivalent to the statement “we use barycentric inertial coordinates” in Newtonian mechanics. BCRS does not define the orientation of the coordinate axes.²

The International Celestial Reference System (ICRS) is a kinematical concept. Its origin is at the solar system barycenter. The ICRS axes are intended to be fixed with respect to space. They are determined based on hundreds of extra-galactic radio sources, mostly quasars, distributed around the sky. The ICRS axes are aligned with the equatorial system based on the J2000.0 mean equator and equinox (see below) to within 17.3 milliarcseconds. The x -axis of the ICRS points in the direction of the mean equinox of J2000.0. The z -axis points very close to the mean celestial north pole of J2000.0, and the y -axis is 90° to the east of the x -axis on the ICRS equatorial plane. So the ICRS is a right-handed rectangular coordinate system. ICRS can be transformed to the equatorial system of J2000.0 by the *frame bias matrix*, which will be discussed below.

It is assumed that those distant extra-galactic radio sources do not rotate with respect to asymptotically flat reference systems like BCRS. In principle this assumption should be checked by testing if the motion of the solar system objects is compatible with the equation of motion based on BCRS, with no Coriolis and centrifugal forces. So far no deviations have been noticed.

However, it is expected that the extra-galactic radio sources should show a secular aberration drift caused by the rotation of the solar system barycenter around the center of Milky Way, and this drift was detected by analyzing decades of the very long baseline interferometry (VLBI) data ([Titov, Lambert & Gontier 2011]). The magnitude of the drift is about 6 micro arcseconds per year, which agrees with the prediction. This effect will need to be taken into account in the future as measurement accuracies continue to improve.

2.2 Geocentric Celestial Reference System (GCRS)

The origin of Geocentric Celestial Reference System (GCRS) is at the center of mass of the Earth. Ignoring general relativistic correction, the GCRS spatial coordinates X^i are related to the BCRS

²IAU 2006 Resolution B2 recommends that the BCRS definition is completed with the following: “For all practical applications, unless otherwise stated, the BCRS is assumed to be oriented according to the ICRS axes. The orientation of the GCRS is derived from the ICRS-oriented BCRS.”

spatial coordinates x^i by

$$X^i = x^i - x_E^i + O((v_E/c)^2), \quad (8)$$

where x_E^i are the BCRS coordinates of Earth's center of mass. Relativistic correction adds terms of order $(v_E/c)^2 \sim 10^{-8} = 0.002''$. The Sun moves along the ecliptic with a rate of about $0.04''$ per second. The Moon moves faster, with a rate of about $0.5''$ per second. Thus ignoring $(v_E/c)^2$ correction will lead to an error of about 0.05 seconds in the computation of the times of 24 solar terms and about 0.004 seconds in the times of moon phases. These errors are much smaller than the one-second accuracy required by the official document [GB/T 33661-2017].

Like BCRS's situation, the orientation of GCRS's axes are unspecified. Here I adopt the recommendaton of IAU 2006 Resolution B2: the axes of BCRS are oriented according to the ICRS axes. Since GCRS's spatial coordinates are defined to be non-rotating with respect to BCRS's spatial coordinates and the $(v_E/c)^2$ terms are neglected, GCRS's axes can also be regarded as being aligned with the ICRS axes.

2.3 Equatorial and Ecliptic Coordinate Systems

The orientation of the coordinate axes described above are fixed in space. This is convenient for describing the positions of stars and planets. However, observations are made on Earth and hence coordinate systems with axes defined by Earth's spin or defined by Earth's orbital plane are often used to describe positions of celestial objects. The coordinate systems whose axes are defined by Earth's spin are called the *equatorial coordinate systems*, and the coordinate system whose axes are defined by Earth's orbital plane are called the *ecliptic coordinate systems*.

2.3.1 Equator, Ecliptic and Equinoxes

The *Celestial Intermediate Pole* (CIP) is the mean rotation axis of the Earth whose motion in space contains aperiodic components as well as periodic components with periods greater than two days. The motion of CIP is described by precession and nutation (see below).

The *true equator* is defined to be the plane perpendicular to the CIP that passes through Earth's center of mass. Thus, the true equator is constantly changing as a result of precession and nutation. The *mean equator* is the moving equator whose motion is prescribed only by precession.

Ecliptic generally refers to Earth's orbital plane projected onto the celestial sphere. However, Earth's orbital plane is changing because of planetary perturbation. To reduce uncertainties in the definition of the ecliptic, the International Astronomical Union (IAU) have recommended that the ecliptic be defined as the plane perpendicular to the mean orbital angular momentum vector of the Earth-Moon barycenter passing through the Sun in the BCRS.

Equator and ecliptic intercepts at two points, called the *vernal equinox* and *autumnal equinox*. The *true equinoxes* are the two points at which the true equator and ecliptic intercepts. The *mean equinoxes* are the two points at which the mean equator and ecliptic intercepts.

2.3.2 Precession, Nutation and Polar Motion

Earth's spin axis changes its orientation in space because of luni-solar and planetary torques on the oblate Earth. Earth's spin axis also moves relative to the crust. This is called the *polar motion*.

The motion of Earth's spin axis is composed of *precession* and *nutation*. Precession is the components that are aperiodic or have periods longer than 100 centuries. Nutation is the components that are of shorter periods and its magnitude is much smaller. Motion with periods shorter than

two days cannot be distinguished from components of polar motion arising from the tidal deformation of the Earth. They are considered as components of polar motion. Therefore, nutation is defined as the periodic components in the motion of Earth's spin axis with periods longer than two days but shorter than about 100 centuries.

The major component of precession is the rotation of Earth's spin axis about the ecliptic pole with a period of about 26,000 years. This causes the vernal equinox to move westward by $50.3''$ per year. The principal period of nutation is 18.6 years, which is caused by the Moon's orbital plane precessing around the ecliptic. The amplitude of nutation is about $9''$. The amplitude of the polar motion is about $0.3''$. Apart from the above mentioned component caused by the tidal deformation of the Earth, there are other components of polar motions, including a 433-day cycle component called the *Chandler wobble*. Polar motion is not relevant in the calculation of moon phases and 24 solar terms because they are not defined using positions relative to a station on Earth's surface but defined by the *geocentric* positions, i.e. positions relative to Earth's center of mass.

In addition to the precession of Earth's spin axis, the orbital plane of the Earth-Moon system around the Sun also moves slowly because of planetary perturbation. Hence the ecliptic moves slowly in space. This is called the *precession of the ecliptic*, to be distinguished from the *precession of the equator*³.

2.3.3 Equatorial “Of Date” Coordinates

Equatorial coordinates are based on the equator and equinox. The x -axis points to the vernal equinox. The y -axis lies in the equatorial plane and is 90° to the east of the x -axis. The z -axis points to the celestial pole. Since equator and equinoxes are moving, an epoch must be specified (e.g. J2000.0) to the coordinate system.

One commonly used equatorial coordinate system is based on the mean equator and equinox of J2000.0 (i.e. mean equator and equinox at TDB noon on January 1, 2000). As mentioned above, there is a small misalignment between the coordinate axes of the ICRS and the axes of the J2000.0 mean equatorial system. The coordinates in the two systems are related by the *frame bias matrix* \mathbf{B} . Let \mathbf{x}_{ICRS} denotes a column vector representing the ICRS coordinates and \mathbf{x}_{2000} denotes a column vector representing coordinates of J2000.0 mean equatorial system. Then

$$\mathbf{x}_{2000} = \mathbf{B}\mathbf{x}_{\text{ICRS}}. \quad (9)$$

The frame bias matrix is given by Equation (4.4) in [Urban & Seidelmann 2013]:

$$\mathbf{B} = \begin{pmatrix} 1 - \frac{1}{2}(d\alpha_0^2 + \xi_0^2) & d\alpha_0 & -\xi_0 \\ -d\alpha_0 - \eta_0\xi_0 & 1 - \frac{1}{2}(d\alpha_0^2 + \eta_0^2) & -\eta_0 \\ \xi_0 - \eta_0d\alpha_0 & \eta_0 + \xi_0d\alpha_0 & 1 - \frac{1}{2}(\eta_0^2 + \xi_0^2) \end{pmatrix}, \quad (10)$$

where $d\alpha_0 = -14.6$ milliarcseconds, $\xi_0 = -16.617$ milliarcseconds, and $\eta_0 = -6.8192$ milliarcseconds. All of them have to be converted to radians. Substituting the numbers to the formula gives

$$\mathbf{B} = \begin{pmatrix} 0.99999999999999425 & -7.078279744 \times 10^{-8} & 8.05614894 \times 10^{-8} \\ 7.078279478 \times 10^{-8} & 0.99999999999999695 & 3.306041454 \times 10^{-8} \\ -8.056149173 \times 10^{-8} & -3.306040884 \times 10^{-8} & 0.999999999999996208 \end{pmatrix}. \quad (11)$$

³Precession of the equator was formerly called the luni-solar precession, and precession of the ecliptic was formerly called the planetary precession. They are renamed because the terminologies are misleading. Planetary perturbation also contributes to the precession of the equator, although the magnitude is much smaller.

To convert \mathbf{x}_{2000} to the coordinates with respect to the true equator and equinox of date requires the multiplication of the precession matrix $\mathbf{P}(t)$ and nutation matrix $\mathbf{N}(t)$:

$$\mathbf{x}_{\text{eq}} = \mathbf{N}(t)\mathbf{P}(t)\mathbf{x}_{2000} = \mathbf{N}(t)\mathbf{P}(t)\mathbf{B}\mathbf{x}_{\text{ICRS}}. \quad (12)$$

The formulas for $\mathbf{P}(t)$ and $\mathbf{N}(t)$ will be given in Section 3 below.

2.3.4 Ecliptic “Of Date” Coordinates

The calculation of the times of moon phases and 24 solar terms requires the positions of the Sun and Moon in ecliptic coordinates of date. The ecliptic coordinate systems are based on the ecliptic and equinox. The x -axis points to the direction of the vernal equinox. The y -axis lies in the ecliptic plane and is 90° to the east of the x -axis. The z -axis points to the ecliptic pole. Therefore, the ecliptic coordinates are related to the equatorial coordinates by a rotation about the x -axis by an angle ϵ , which is called the *obliquity of the ecliptic* and is the angle between the ecliptic pole and the CIP. Note that $\epsilon = \epsilon(t)$ is a function of time because of precession and nutation. The value of ϵ can be computed by equation (30) below. Let \mathbf{x}_{eq} be the column vector representing the equatorial coordinates with respect to the true equator and equinox of date, and \mathbf{x}_{ec} be the column vector representing the ecliptic coordinates with respect to the ecliptic and true equinox of date. Then

$$\mathbf{x}_{\text{ec}} = \mathbf{R}_1(\epsilon(t))\mathbf{x}_{\text{eq}} = \mathbf{R}_1(\epsilon(t))\mathbf{N}(t)\mathbf{P}(t)\mathbf{B}\mathbf{x}_{\text{ICRS}}, \quad (13)$$

where the rotation matrix is

$$\mathbf{R}_1(\epsilon(t)) = \begin{pmatrix} 1 & 0 & 0 \\ 0 & \cos \epsilon(t) & \sin \epsilon(t) \\ 0 & -\sin \epsilon(t) & \cos \epsilon(t) \end{pmatrix}. \quad (14)$$

The *ecliptic longitude* λ is defined as $\arg(x_{\text{ec}} + iy_{\text{ec}})$, where $\arg(z)$ denotes the argument of the complex number z . In other words, $\lambda = \tan^{-1}(y_{\text{ec}}/x_{\text{ec}})$ with the angle in the appropriate quadrant. In many programming languages, there is an arctangent function (e.g. `atan2` in FORTRAN, C and python) that returns the angle in the correct quadrant.

3 Precession and Nutation

3.1 Precession Matrix

Denote $\mathbf{X} = (X \ Y \ Z)^T$ the equatorial coordinates based on the mean equator and equinox at TDB time t and $\mathbf{X}_0 = (X_0 \ Y_0 \ Z_0)^T$ the equatorial coordinates based on the mean equator and equinox at J2000.0, where the superscript T denotes transpose. So \mathbf{X} and \mathbf{X}_0 are column vectors, and they are related by a 3D rotation described by the precession matrix $\mathbf{P}(t)$:

$$\mathbf{X} = \mathbf{P}(t)\mathbf{X}_0. \quad (15)$$

In August 2006, the 26th General Assembly for the International Astronomical Union passed a resolution recommending that the P03 precession theory of [Capitaine et al 2003] be used for the precession matrix. This model is referred to as the IAU 2006 precession theory. According to this theory, the precession matrix is given by

$$\mathbf{P}(t) = \mathbf{R}_3(\chi_A)\mathbf{R}_1(-\omega_A)\mathbf{R}_3(-\psi_A)\mathbf{R}_1(\epsilon_0), \quad (16)$$

where the rotation matrix \mathbf{R}_1 is given by equation (14) above and the rotation matrix \mathbf{R}_3 is given by

$$\mathbf{R}_3(\theta) = \begin{pmatrix} \cos \theta & \sin \theta & 0 \\ -\sin \theta & \cos \theta & 0 \\ 0 & 0 & 1 \end{pmatrix}. \quad (17)$$

The angle $\epsilon_0 = 84381.406''$ is the inclination angle between the J2000.0 ecliptic and J2000.0 mean equator. The angles ψ_A , ω_A and χ_A can be found in equation (5.7) in [Kaplan 2005] or (5.39) and (5.40) in [IERS Conventions 2010]. They are given by

$$\begin{aligned} \psi_A &= 5038.481507''T - 1.0790069''T^2 - 0.00114045''T^3 + 0.000132851''T^4 - 9.51'' \times 10^{-8}T^5 \\ \omega_A &= 84381.406'' - 0.025754''T + 0.0512623''T^2 - 0.00772503''T^3 - 4.67'' \times 10^{-7}T^4 \\ &\quad + 3.337'' \times 10^{-7}T^5 \\ \chi_A &= 10.556403''T - 2.3814292''T^2 - 0.00121197''T^3 + 0.000170663''T^4 - 5.60'' \times 10^{-8}T^5, \end{aligned} \quad (18)$$

where $T = (JD - 2451545)/36525$ is the Julian century from J2000.0 and JD is the TDB Julian date number. The result of the matrix multiplication in equation (16) is also written out explicitly in equation (5.10) in [Kaplan 2005]:

$$\begin{aligned} P_{11}(t) &= C_4C_2 - S_2S_4C_3 \\ P_{12}(t) &= C_4S_2C_1 + S_4C_3C_2C_1 - S_1S_4S_3 \\ P_{13}(t) &= C_4S_2S_1 + S_4C_3C_2S_1 + C_1S_4S_3 \\ P_{21}(t) &= -S_4C_2 - S_2C_4C_3 \\ P_{22}(t) &= -S_4S_2C_1 + C_4C_3C_2C_1 - S_1C_4S_3 \\ P_{23}(t) &= -S_4S_2S_1 + C_4C_3C_2S_1 + C_1C_4S_3 \\ P_{31}(t) &= S_2S_3 \\ P_{32}(t) &= -S_3C_2C_1 - S_1C_3 \\ P_{33}(t) &= -S_3C_2S_1 + C_3C_1 \end{aligned} \quad (19)$$

where

$$\begin{aligned} S_1 &= \sin \epsilon_0 & C_1 &= \cos \epsilon_0 \\ S_2 &= \sin(-\psi_A) & C_2 &= \cos(-\psi_A) \\ S_3 &= \sin(-\omega_A) & C_3 &= \cos(-\omega_A) \\ S_4 &= \sin \chi_A & C_4 &= \cos \chi_A \end{aligned} \quad (20)$$

3.2 Nutation Matrix

Nutation is computed according to the IAU 2000A Theory of Nutation with slight IAU 2006 adjustments. To construct the nutation matrix $\mathbf{N}(t)$, we need to first compute the following 14 arguments given by equations (5.43) and (5.44) in [IERS Conventions 2010].

$$\begin{aligned} F_1 \equiv l &= \text{Mean Anomaly of the Moon} \\ &= 134.96340251^\circ + 1717915923.2178''T + 31.8792''T^2 \\ &\quad + 0.051635''T^3 - 0.00024470''T^4 \end{aligned}$$

$$\begin{aligned} F_2 \equiv l' &= \text{Mean Anomaly of the Sun} \\ &= 357.52910918^\circ + 129596581.0481''T - 0.5532''T^2 \end{aligned}$$

$$+0.000136''T^3 - 0.00001149''T^4$$

$$\begin{aligned} F_3 \equiv F &= L - \Omega = \text{Mean Longitude of the Moon} - \Omega \\ &= 93.27209062^\circ + 1739527262.8478''T - 12.7512''T^2 \\ &\quad - 0.001037''T^3 + 0.00000417''T^4 \end{aligned} \quad (21)$$

$$\begin{aligned} F_4 \equiv D &= \text{Mean Elongation of the Moon from the Sun} \\ &= 297.85019547^\circ + 1602961601.2090''T - 6.3706''T^2 \\ &\quad + 0.006593''T^3 - 0.00003169''T^4 \end{aligned}$$

$$\begin{aligned} F_5 \equiv \Omega &= \text{Mean Longitude of the Ascending Node of the Moon} \\ &= 125.04455501^\circ - 6962890.5431''T + 7.4722''T^2 \\ &\quad + 0.007702''T^3 - 0.00005939''T^4 \end{aligned}$$

The rest of the arguments are the mean longitudes of the 8 planets and general precession. They are given in radians as

$$\begin{aligned} F_6 &\equiv L_{\text{Mercury}} = 4.402608842 + 2608.7903141574T \\ F_7 &\equiv L_{\text{Venus}} = 3.176146697 + 1021.3285546211T \\ F_8 &\equiv L_{\text{Earth}} = 1.753470314 + 628.3075849991T \\ F_9 &\equiv L_{\text{Mars}} = 6.203480913 + 334.0612426700T \\ F_{10} &\equiv L_{\text{Jupiter}} = 0.599546497 + 52.9690962641T \\ F_{11} &\equiv L_{\text{Saturn}} = 0.874016757 + 21.3299104960T \\ F_{12} &\equiv L_{\text{Uranus}} = 5.481293872 + 7.4781598567T \\ F_{13} &\equiv L_{\text{Neptune}} = 5.311886287 + 3.8133035638T \\ F_{14} &\equiv p_A = 0.02438175T + 0.00000538691T^2 \end{aligned} \quad (22)$$

Next, the nutation in longitude $\Delta\psi$ and nutation in obliquity $\Delta\epsilon$ are given by the expressions

$$\Delta\psi = \sum_{i=1}^{1320} [A_i \sin \theta_i^A + A_i'' \cos \theta_i^A] + \sum_{i=1}^{38} [A_i' \sin \theta_i^{A'} + A_i''' \cos \theta_i^{A'}]T \quad (23)$$

$$\Delta\epsilon = \sum_{i=1}^{1037} [B_i \cos \theta_i^B + B_i'' \sin \theta_i^B] + \sum_{i=1}^{19} [B_i' \cos \theta_i^{B'} + B_i''' \sin \theta_i^{B'}]T, \quad (24)$$

where the arguments of the sine and cosine functions are given by

$$\theta_i^A = \sum_{j=1}^{14} C_{ij}^A F_j, \quad \theta_i^{A'} = \sum_{j=1}^{14} C_{ij}^{A'} F_j, \quad \theta_i^B = \sum_{j=1}^{14} C_{ij}^B F_j, \quad \theta_i^{B'} = \sum_{j=1}^{14} C_{ij}^{B'} F_j. \quad (25)$$

The coefficients A_i , A_i' , A_i'' , A_i''' , C_{ij}^A and $C_{ij}^{A'}$ are listed in the table on the IERS ftp site <ftp://tai.bipm.org/iers/conv2010/chapter5/tab5.3a.txt>. Values of A_i and A_i'' are given in the

second and third columns in the first 1320 rows; A'_i and A'''_i are given in the second and third columns in the last 38 rows; C_{ij}^A are given in columns 4 to 17 in the first 1320 rows; $C_{ij}^{A'}$ are given in columns 4 to 17 in the last 38 rows. Coefficients B_i , B'_i , B''_i , B'''_i , C_{ij}^B and $C_{ij}^{B'}$ are given in the table on the IERS ftp site <ftp://tai.bipm.org/iers/conv2010/chapter5/tab5.3b.txt>. To make sure the tables are read correctly, I list the first few terms for $\Delta\psi$ and $\Delta\epsilon$:

$$\begin{aligned}\Delta\psi = & -17.20642418'' \sin \Omega + 0.003386'' \cos \Omega \\ & -1.31709122'' \sin(2F - 2D + 2\Omega) - 0.0013696'' \cos(2F - 2D + 2\Omega) + \dots\end{aligned}\quad (26)$$

$$\begin{aligned}\Delta\epsilon = & 0.0015377'' \sin \Omega + 9.2052331'' \cos \Omega \\ & -0.0004587'' \sin(2F - 2D + 2\Omega) + 0.5730336'' \cos(2F - 2D + 2\Omega) + \dots\end{aligned}\quad (27)$$

The nutation matrix \mathbf{N} is given by the expression

$$\mathbf{N} = \mathbf{R}_1(-\epsilon)\mathbf{R}_3(-\Delta\psi)\mathbf{R}_1(\epsilon_A), \quad (28)$$

where ϵ_A is the mean obliquity of the ecliptic of date (inclination of the ecliptic of date with respect to the mean equator of date) and ϵ is the true obliquity of the ecliptic of date (inclination of the ecliptic of date with respect with the true equator of date). They are given by the equations

$$\begin{aligned}\epsilon_A = & 84381.406'' - 46.836769''T - 0.0001831''T^2 + 0.00200340''T^3 \\ & -0.000000576''T^4 - 0.0000000434''T^5\end{aligned}\quad (29)$$

$$\epsilon = \epsilon_A + \Delta\epsilon \quad (30)$$

If we are only interested in computing the components of the position and velocity associated with the ecliptic and true equinox of date, the computation can be simplified. From equation (13) we see that the transformation involves $\mathbf{R}_1(\epsilon)\mathbf{N}$. It follows from (28) and $\mathbf{R}_1(\epsilon)\mathbf{R}_1(-\epsilon) = I$ (identity matrix) that

$$\mathbf{R}_1(\epsilon)\mathbf{N} = \mathbf{R}_3(-\Delta\psi)\mathbf{R}_1(\epsilon_A) = \begin{pmatrix} \cos \Delta\psi & -\sin \Delta\psi \cos \epsilon_A & -\sin \Delta\psi \sin \epsilon_A \\ \sin \Delta\psi & \cos \Delta\psi \cos \epsilon_A & \cos \Delta\psi \sin \epsilon_A \\ 0 & -\sin \epsilon_A & \cos \epsilon_A \end{pmatrix}. \quad (31)$$

This means that it is not necessary to calculate the nutation in obliquity $\Delta\epsilon$.

The nutation in longitude $\Delta\psi$ is expressed by a sum over 1000 terms. An accuracy of 0.04'' is necessary in order to compute the times of 24 solar terms to one-second accuracy required by the official document [GB/T 33661-2017]. It is not necessary to include all 1000+ terms since many of them are very small. One possibility is to use the IAU 2000B nutation model, which is an abridged nutation model. IAU 2000B model contains fewer than 80 terms and its deviation from IAU 2000A model is less than 1 milliarcsecond during the period 1995–2050. However, I include all of the 1000+ terms in IAU 2000A model in the calculation. Even though they substantially slow down the code, it still takes only about 17 seconds to compute the times of all moon phases and solar terms from 1600 to 3500 using my somewhat dated computer at home 6 seconds to compute the times of all moon phases and solar terms from 1600 to 3500 using my computer at home. This is still tolerable considering that the computation of the TDB times only needs to be carried out once for a given ephemeris. As will be discussed in Section 7, nutation is only required in the computation of 24 solar terms.

4 Jet Propulsion Laboratory Development Ephemeris

Jet Propulsion Laboratory (JPL) development ephemeris is often abbreviated as JPL DE(number) or just DE(number). It refers to a particular ephemeris model developed by the JPL based on numerical integration. The main purpose of the ephemerides is for spacecraft navigation and astronomy. JPL has been improving their ephemerides since 1960s. The DE ephemerides are among the most accurate ephemerides currently available. I use DE431 in my calculation of moon phases and 24 solar terms for my Chinese calendar website. DE430 and DE431 ([Folkner et al 2014]) were created in 2013. DE430 has been the basis of the *Astronomical Almanac* since 2015. DE431 is currently used on JPL’s HORIZONS Web-Interface to generate ephemerides for solar-system bodies.

DE430 and DE431 take into account gravitational perturbations from 343 relatively large-mass asteroids. General relativistic effects are included by using dynamical equations derived from a parameterized post-Newtonian n -body metric. Additional accelerations arising from non-spherical effects of extended bodies including the Earth, Moon and Sun are also included.

The major difference between DE430 and DE431 is that DE430 includes a damping term between the Moon’s liquid core and solid mantle that gives the best fit to observation data but that is not suitable for backward integration of more than a few centuries. DE431 is similar to DE430 but without the core/mantle damping term, so the lunar position is less accurate than in DE430 for times near the current epoch, but is more suitable for times more than a few centuries in the past. DE431 covers years from -13,200 to +17,191, whereas DE430 covers years from 1550 to 2650.

Since the release of DE430 and DE431, JPL had minor upgrades to their ephemerides, releasing DE432, DE433, ..., DE436 and DE438. Each of these interim ephemerides was generated for a specific flight project. In 2020, JPL generated two general-purpose ephemerides DE440 and DE441 ([Park et al 2021]). These two ephemerides replace DE430 and DE431 and their precursors. The integration method of DE440 and DE441 is the same as that of DE430 and DE431, with the addition of seven years of new data and with improved dynamical models and data calibration.

In DE440 and DE441, orbits of the inner planets are determined from Mercury Surface Space Environment Geochemistry and Ranging (MESSENGER), Venus Express and Mars-orbiting spacecraft. Moon’s data are obtained from lunar laser ranging. The accuracy of Jupiter’s orbit has improved substantially from the radio range and Very Long Baseline Array (VLBA) data of the Juno spacecraft. Saturn’s orbit has been improved by radio range and VLBA data of the Cassini spacecraft, with improved estimation of the spacecraft orbit. The orbits of Uranus and Neptune are determined by astrometry and radio range measurements to the Voyager flybys. Pluto’s orbit is now determined by stellar occultations reduced against the Gaia star catalog.

DE440 and DE441 also added several new dynamical models. In particular, they include perturbations from 30 individual Kuiper belt objects (KBOs) and a circular ring representing the rest of the Kuiper belt, modeled as 36 point masses with an equal mass located at 44 AU in the ecliptic. The Lense-Thirring effect from the Sun’s angular momentum has also been added. This effect is small but is important for fitting the MESSENGER range data. It also slightly modifies Mercury’s perihelion precession rate. The Lieske (1979) precession model is now replaced by the precession model of [Vondrák et al 2011] to compute the orientation of Earth. The effect of geodetic precession on lunar librations is added on the Moon and the solar radiation pressure force is added on the Earth-Moon system.

As in the case of DE430 and DE431, DE440 includes the core/mantle damping term but DE441 does not. The time span of DE440 is from 1550 to 2650, whereas DE441 covers -13200–17191.

4.1 Downloading and Reading the JPL Ephemerides

JPL’s DE ephemerides are released in binary files containing the Chebyshev polynomials fit to the rectangular coordinates of the positions of the Sun, Moon and planets. The coefficients of Chebyshev polynomials have a time dependence, which is typically broken into 32-day intervals. The number of Chebyshev coefficients depends on the object. It is determined so that the deviations between the interpolated coordinate values and values provided by the ephemerides are less than 0.5 millimeters ([Newhall 1989]), or 3.3×10^{-15} astronomical units. This level of interpolation error is smaller than the estimated error of the numerical integration used to create the ephemerides. Thus the interpolation result can be regarded as the same as the numerical integration result.

I downloaded the DE files from JPL’s ftp site `ftp://ssd.jpl.nasa.gov/pub/eph/planets/Linux/`. The main files are in binary format and require software to read and to perform interpolation. I use Project Pluto’s C source code for reading the JPL ephemerides and performing computation. For each DE ephemeris, JPL’s ftp site provides a file for checking values of the position and velocity coordinates of different solar system objects at thousands or even tens of thousands of different TDB times.

I downloaded the ephemerides DE405, DE406, DE430, DE431, DE440 and DE441 from JPL’s ftp site. The sizes of the binary files are 53.3MB for DE405, 190MB for DE406, 85.5MB for DE430, 2.6GB for DE431, 97.5MB for DE440 and 2.6GB for DE441. For each ephemeris I downloaded, I went through the data in the check file and confirmed that Project Pluto’s C code reproduces the data in the file to floating-point roundoff precision. That is, the relative error is smaller than $2^{-53} \approx 1.11 \times 10^{-16}$.

4.2 Computing the Geometric Position and Velocity in GCRS

Project Pluto’s software contains a function that can be used to calculate the rectangular coordinates of the positions and velocities of the Sun, Moon, and planets relative to a specified object at any given TDB time using the coefficients of the Chebyshev polynomials from the appropriate time interval. The axes of the rectangular coordinate system are aligned with that of the ICRS. The raw data of the ephemerides are the rectangular coordinates of the positions of solar system objects in BCRS (except for the Moon in which rectangular coordinates of the geocentric positions are calculated). I denote the rectangular coordinates of the position (in BCRS) of a particular object at a given TDB time t by the vector $\mathbf{x}(t)$, and the velocity by $\mathbf{v}(t)$. The position and velocity of the object relative to a target object are simply computed from $\mathbf{X}(t) = \mathbf{x}(t) - \mathbf{x}_t(t)$ and $\mathbf{V}(t) = \mathbf{v}(t) - \mathbf{v}_t(t)$, where $\mathbf{x}_t(t)$ and $\mathbf{v}_t(t)$ are respectively the position and velocity of the target object in BCRS. For the calculation of moon phases and 24 solar terms, the relevant target is the Earth. The resulting vectors \mathbf{X} and \mathbf{V} represent the rectangular coordinates of the geocentric position and velocity of the object. These are called the *geometry* position and velocity. They need to be converted to the *apparent* position and velocity by taking into account the combined effect of light-time correction and aberration of light.

5 Light-Time Correction and Aberration of Light

Since the speed of light is finite, the observed position of an object is the object’s *retarded position*, i.e. the position at which light emitted earlier has just reached the observer. This is called the *light-time correction*. Let $\mathbf{x}(t)$ be the BCRS geometric position of the object at time t , and $\mathbf{x}_E(t)$

be Earth's BCRS geometric position at time t . Then the retarded GCRS position at time t is $\mathbf{X}_r(t) = \mathbf{x}(t_r) - \mathbf{x}_E(t)$, where the retarded time t_r satisfies the equation

$$t_r = t - \frac{|\mathbf{x}(t_r) - \mathbf{x}_E(t)|}{c} \quad (32)$$

and $c = 299792.458$ km/s is the speed of light. This formula ignores the general relativistic effect caused by spacetime curvature. The effect adds a correction of only $< 10^{-4}$ s for the Sun and $\sim 10^{-8}$ s for the Moon. Note that the retarded time t_r appears on both sides of equation (32). This means that it has to be solved iteratively. However, for the Sun and Moon, it is sufficient to use

$$t_r \approx t - \frac{|\mathbf{x}(t) - \mathbf{x}_E(t)|}{c}. \quad (33)$$

By making this approximation, the error in $\mathbf{X}_r(t)$ is of order $(v/c)^2$, where $v = |\dot{\mathbf{x}}|$ is the speed of the object in BCRS. Since the Sun contains 99.86% of total mass in the solar system, the motion of the Sun in BCRS is very small (see Appendix A). Thus, $\mathbf{x}(t_r) \approx \mathbf{x}(t)$ for the Sun and $(v/c)^2$ is very tiny for the Sun. The Moon's orbital speed around the Earth is about 1 km/s, which is much smaller than the orbital speed of the Earth-Moon barycenter (about 30 km/s). Hence the speed of the Moon in BCRS is about 30 km/s and $(v/c)^2 \sim 10^{-8}$ for the Moon. The error associated with the Moon's position is therefore only $0.002''$ and can be safely ignored.

Aberration of light also arises from the finite speed of light. Suppose an observer sees an object in the direction \mathbf{n} , the direction of the object relative to another observer at the same position but moving with velocity \mathbf{v} will be in a direction \mathbf{n}' . The unit vectors \mathbf{n} and \mathbf{n}' are related by the Lorentz transformation of special relativity⁴ (see Appendix C):

$$\mathbf{n}' = \frac{\gamma^{-1}\mathbf{n} + \boldsymbol{\beta} + (\mathbf{n} \cdot \boldsymbol{\beta})\boldsymbol{\beta}/(1 + \gamma^{-1})}{1 + \boldsymbol{\beta} \cdot \mathbf{n}}, \quad (34)$$

where $\boldsymbol{\beta} = \mathbf{v}/c$ and $\gamma = 1/\sqrt{1 - (v/c)^2}$. In our case, $\mathbf{n} = \mathbf{X}_r/|\mathbf{X}_r|$ and $\mathbf{v} = \dot{\mathbf{x}}_E$ is Earth's velocity in BCRS. Since Earth's orbital speed in BCRS is about 30 km/s, it is sufficient to calculate the aberration of light to first order in v/c . When expanded to order v/c , the expression in the Lorentz transformation is the same as in Newtonian kinematics:

$$\mathbf{n}' = \frac{\mathbf{n} + \boldsymbol{\beta}}{|\mathbf{n} + \boldsymbol{\beta}|}. \quad (35)$$

Here $\boldsymbol{\beta} = \dot{\mathbf{x}}_E/c$. This is called the *annual aberration* because $\boldsymbol{\beta}$ changes directions with a period of one year as the Earth moves around the Sun. There is another aberration effected called the *diurnal aberration*, which is caused by the rotation of the Earth. However, diurnal aberration only affects the positions of an object observed on Earth's surface. It is irrelevant to the calculation of moon phases and solar terms because they are defined by the geocentric positions of the Sun and Moon, which are unaffected by the diurnal aberration.

The aberration of light shifts an object's position by an amount of $\sim v_E/c \approx 10^{-4} \approx 20.5''$. Failure to take into account the aberration effect will result in an error in the times of the 24 solar terms by about 8 minutes, which is about the time it takes for light to travel from the Sun to Earth. This is not a coincidence. As explained in Section 7.2.3.5 of [Urban & Seidelmann 2013],

⁴General relativistic effects, such as gravitational deflection of light, are ignored since the correction is very small for the Sun and Moon

there is a simple method to calculate the combined effect of light-time correction and aberration of light, also known as the *planetary aberration*, to first order in v/c . I provide a derivation here. It follows from $\mathbf{n} = \mathbf{X}_r/|\mathbf{X}_r|$ and equation (35) that

$$\begin{aligned}
\mathbf{n}' &\propto \frac{\mathbf{X}_r}{|\mathbf{X}_r|} + \frac{\dot{\mathbf{x}}_E}{c} \\
&= \frac{\mathbf{x}(t_r) - \mathbf{x}_E(t)}{|\mathbf{x}(t_r) - \mathbf{x}_E(t)|} + \frac{\dot{\mathbf{x}}_E}{c} \\
&\propto \mathbf{x}(t_r) - \left[\mathbf{x}_E(t) - \frac{|\mathbf{x}(t_r) - \mathbf{x}_E(t)|}{c} \dot{\mathbf{x}}_E \right] \\
&\approx \mathbf{x}(t_r) - \mathbf{x}_E \left(t - \frac{|\mathbf{x}(t_r) - \mathbf{x}_E(t)|}{c} \right) \\
&= \mathbf{x}(t_r) - \mathbf{x}_E(t_r).
\end{aligned} \tag{36}$$

Hence to first order in v/c , the combined effect of light-time correction and aberration of light results in the *proper position* given by

$$\mathbf{X}_{\text{proper}}(t) = \mathbf{x}(t_r) - \mathbf{x}_E(t_r). \tag{37}$$

For the Sun, t_r is the time it takes for light to travel from the Sun to Earth. This is the reason that the aberration effect causes a correction of about 8 minutes. For the Moon, $t_r = 1.3$ seconds, which can not be neglected if we want to meet the one-second accuracy requirement stated in the document [GB/T 33661-2017]. Equation (37) is very convenient in calculating the combined effect of light-time correction and aberration of light since there is a function in Project Pluto's software that can be used to compute the geometric position $\mathbf{x} - \mathbf{x}_E$ for any solar system object at any given TDB time. Equation (37) says the proper position at time t is the same as the geometric GCRS position at time t_r .

In addition to the proper position, it is also useful to compute its time derivative. Taking the time derivative of equation (37) yields

$$\dot{\mathbf{X}}_{\text{proper}}(t) = [\dot{\mathbf{x}}(t_r) - \dot{\mathbf{x}}_E(t_r)] \frac{dt_r}{dt}. \tag{38}$$

Denote $D(t_r) = |\mathbf{x}(t_r) - \mathbf{x}_E(t)|$ as the retarded distance and using (32), I obtain

$$\frac{dt_r}{dt} = 1 - \frac{\dot{D}(t_r)}{c} \frac{dt_r}{dt} \Rightarrow \frac{dt_r}{dt} = \frac{1}{1 + v_r(t_r)/c}, \tag{39}$$

where $v_r = dD/dt$ is the radial velocity of the object relative to Earth. Equation (38) can be written as

$$\dot{\mathbf{X}}_{\text{proper}}(t) = \frac{\dot{\mathbf{x}}(t_r) - \dot{\mathbf{x}}_E(t_r)}{1 + v_r(t_r)/c} \tag{40}$$

The denominator in the above expression is the cause of the apparent superluminal motion of jets in some active galaxies: if a jet moving close to the speed of light is moving at a very small angle towards the observer, $1 + v_r/c \ll 1$ and it is possible to have the apparent tangential speed greater than the speed of light. However, v_r/c is negligible for the Sun and Moon because both Earth's orbit around the Sun and Moon's orbit around Earth are nearly circular. The radial speed

$|v_r| \sim 0.5$ km/s for the Sun (see Appendix A) and $|v_r| \sim 0.05$ km/s for the Moon (see Appendix B). Hence the fractional error in ignoring the v_r/c term is of order 10^{-6} for the Sun and 10^{-7} for the Moon. As will be explained in Section 7, this error has almost no effect on the accuracy of the times of moon phases and 24 solar term. I therefore ignore it and set

$$\dot{\mathbf{X}}_{\text{proper}}(t) = \dot{\mathbf{x}}(t_r) - \dot{\mathbf{x}}_{\mathbf{E}}(t_r) = \mathbf{v}(t_r) - \mathbf{v}_{\mathbf{E}}(t_r). \quad (41)$$

This is also a very convenient equation to compute $\dot{\mathbf{X}}_{\text{proper}}$ since there is a function in Project Pluto's software that can be used to compute $\mathbf{v} - \mathbf{v}_{\mathbf{E}}$ for any solar system object at any given TDB time. Equation (41) says the proper velocity at time t is equal to the geometric GCRS velocity at time t_r .

6 Apparent Geocentric Longitude

The apparent geocentric longitude of the Sun and Moon are crucial in the computation of the times of moon phases and 24 solar terms. The longitude can be computed by combining the equations in Sections 2, 3 and 5. Here are the steps of the calculation for a given TDB time t :

1. Compute the geometric position of the object (Sun or Moon) in GCRS by $\mathbf{X}_{\text{geometric}}(t) = \mathbf{x}(t) - \mathbf{x}_{\mathbf{E}}(t)$, where \mathbf{x} is the BCRS position of the object and $\mathbf{x}_{\mathbf{E}}$ is the BCRS position of the Earth. This can be computed directly using the C function provided by Project Pluto's package.
2. Compute the retarded time approximately using $t_r \approx t - |\mathbf{X}_{\text{geometric}}(t)|/c$.
3. Compute the proper position using the equation $\mathbf{X}_{\text{proper}}(t) \approx \mathbf{x}(t_r) - \mathbf{x}_{\mathbf{E}}(t_r)$, which can also be computed directly using Project Pluto's C function. The resulting vector gives the components in the GCRS coordinate system. Recall that the origin of the GCRS is at the geocenter and its axes are aligned with those of the ICRS.
4. Calculate the precession matrix $\mathbf{P}(t)$ using equations (18), (19) and (20). Calculate the matrix $\mathbf{R}_1(\epsilon(t))\mathbf{N}(t)$ using equations (21)–(23), (25), (29) and (31).
5. Convert the proper position $\mathbf{X}_{\text{proper}}(t)$ to the apparent geocentric position in coordinates associated with the ecliptic and true equinox of date using the equation

$$\mathbf{X}_{\text{ec}}(t) = \mathbf{R}_1(\epsilon(t))\mathbf{N}(t)\mathbf{P}(t)\mathbf{B}\mathbf{X}_{\text{proper}}(t), \quad (42)$$

where the frame bias matrix \mathbf{B} is given by equation (11).

6. Calculate the apparent geocentric longitude using $\lambda = \arg(X_{\text{ec}} + iY_{\text{ec}})$. That is, $\lambda = \tan^{-1}(Y_{\text{ec}}/X_{\text{ec}})$ in the appropriate quadrant.

It is also useful to calculate the time derivative of λ . Differentiating $\lambda(t) = \tan^{-1}[Y_{\text{ec}}(t)/X_{\text{ec}}(t)]$ yields

$$\dot{\lambda}(t) = \frac{X_{\text{ec}}\dot{Y}_{\text{ec}} - Y_{\text{ec}}\dot{X}_{\text{ec}}}{X_{\text{ec}}^2 + Y_{\text{ec}}^2}. \quad (43)$$

The time derivatives \dot{X}_{ec} and \dot{Y}_{ec} are obtained by differentiating equation (42) with respect to t :

$$\dot{\mathbf{X}}_{\text{ec}}(t) = \mathbf{R}_1(\epsilon(t))\mathbf{N}(t)\mathbf{P}(t)\mathbf{B}\dot{\mathbf{X}}_{\text{proper}}(t) + \frac{d}{dt}[\mathbf{R}_1(\epsilon(t))\mathbf{N}(t)\mathbf{P}(t)]\mathbf{B}\mathbf{X}_{\text{proper}}(t). \quad (44)$$

The first term arises from the fact that the object is moving relative to Earth; the second term arises from the fact that the coordinate axes associated with the ecliptic and true equinox of date are moving because of precession and nutation. Obviously the first term is the dominant term and the second term can be ignored. Hence,

$$\dot{\mathbf{X}}_{\text{ec}}(t) \approx \mathbf{R}_1(\epsilon(t))\mathbf{N}(t)\mathbf{P}(t)\mathbf{B}\dot{\mathbf{X}}_{\text{proper}}(t) = \mathbf{R}_1(\epsilon(t))\mathbf{N}(t)\mathbf{P}(t)\mathbf{B}[\mathbf{v}(t_r) - \mathbf{v}_E(t_r)]. \quad (45)$$

The vector $\mathbf{v}(t_r) - \mathbf{v}_E(t_r)$ can be computed directly using Project Pluto's C function.

Let's perform an order of magnitude estimate of the error in dropping the second term. The sidereal period of the Earth around the Sun is 365.2564 days. This means that the Sun completes a full circle as seen on Earth in the GCRS coordinates in 365.2564 days. So in one day, the Sun moves, on average, about $360^\circ/365.2564 \approx 1^\circ$. Hence $|\dot{\mathbf{X}}_{\text{proper}}|/|\mathbf{X}_{\text{proper}}| \approx 1^\circ/\text{day}$ for the Sun. The Moon's sidereal period around Earth is 27.3217 days. Similar calculation shows $|\dot{\mathbf{X}}_{\text{proper}}|/|\mathbf{X}_{\text{proper}}| \approx 13^\circ/\text{day}$ for the Moon. The major component of precession is the westward motion of the vernal equinox at a rate of $50.3''/\text{year}$, which is about $0.14''/\text{day}$. Hence, $|\dot{\mathbf{P}}| \sim 0.14''/\text{day}$. Here $|\dot{\mathbf{P}}|$ means the (maximum) magnitude of the components in the $\dot{\mathbf{P}}$ matrix. The major component of nutation is the 18.6 year cycle caused by Moon's orbital plane precessing around the ecliptic. This is represented by the first term in equation (26). So $|d(\mathbf{R}_1(\epsilon)\mathbf{N})/dt| \sim 17.2''|\dot{\Omega}|$ and from equation (21) we have $|\dot{\Omega}| \approx 7000000''/\text{century} \approx 10^{-3} \text{ rad/day}$. Hence $|d(\mathbf{R}_1(\epsilon)\mathbf{N})/dt| \sim 0.02''/\text{day}$. Thus, not surprisingly precession is the dominant component in the second term, but $|\dot{\mathbf{P}}|/|\mathbf{X}_{\text{proper}}| \sim 4 \times 10^{-5}$ for the Sun and $\sim 3 \times 10^{-6}$ for the Moon. Therefore, dropping the second term introduces a fractional error of order 4×10^{-5} for the Sun and 3×10^{-6} for the Moon. As will be explained in the next section, this error has almost no effect on the accuracy in the times of the moon phases and 24 solar terms.

7 Computation of the TDB Times of Moon Phases and 24 Solar Terms

The 24 solar terms are defined when the apparent geocentric longitude of the Sun reaches integer multiples of 15° or $\pi/12$ radians. Hereafter, all angles are assumed to be in radians. New moon (lunar conjunction) is defined when the apparent geocentric longitude of the Moon λ_M is equal to the apparent geocentric longitude of the Sun λ_S . First quarter is defined when $P(\lambda_M - \lambda_S) = \pi/2$; full moon is defined when $P(\lambda_M - \lambda_S) = -\pi$; third quarter is defined when $P(\lambda_M - \lambda_S) = -\pi/2$. Here the function P is defined as

$$P(x) \equiv x - 2\pi \left\lfloor \frac{x + \pi}{2\pi} \right\rfloor \quad (46)$$

and $[x]$ means the largest integer less than or equal to x . Thus, the operator $\lfloor \cdot \rfloor$ is the same as the `floor` function in C and python. The function P simply adds an integer multiples of 2π to bring the argument into the interval $[-\pi, \pi)$. Computation of the times of moon phases and 24 solar terms therefore boils down to finding the roots of $f(t) = 0$. The function f is listed in the tables below for computing the moon phases and 24 solar terms. Note that both λ_S and λ_M are functions of t .

Moon Phase	Function f
new moon	$P(\lambda_M - \lambda_S)$
first quarter	$P(\lambda_M - \lambda_S - \pi/2)$
full moon	$P(\lambda_M - \lambda_S - \pi)$
third quarter	$P(\lambda_M - \lambda_S + \pi/2)$

Solar Term	Function f	Solar Term	Function f
J1 (立春)	$P(\lambda_S + \pi/4)$	Z1 (雨水)	$P(\lambda_S + \pi/6)$
J2 (驚蟄)	$P(\lambda_S + \pi/12)$	Z2 (春分)	$P(\lambda_S)$
J3 (清明)	$P(\lambda_S - \pi/12)$	Z3 (穀雨)	$P(\lambda_S - \pi/6)$
J4 (立夏)	$P(\lambda_S - \pi/4)$	Z4 (小滿)	$P(\lambda_S - \pi/3)$
J5 (芒種)	$P(\lambda_S - 5\pi/12)$	Z5 (夏至)	$P(\lambda_S - \pi/2)$
J6 (小暑)	$P(\lambda_S - 7\pi/12)$	Z6 (大暑)	$P(\lambda_S - 2\pi/3)$
J7 (立秋)	$P(\lambda_S - 3\pi/4)$	Z7 (處暑)	$P(\lambda_S - 5\pi/6)$
J8 (白露)	$P(\lambda_S - 11\pi/12)$	Z8 (秋分)	$P(\lambda_S - \pi)$
J9 (寒露)	$P(\lambda_S + 11\pi/12)$	Z9 (霜降)	$P(\lambda_S + 5\pi/6)$
J10 (立冬)	$P(\lambda_S + 3\pi/4)$	Z10 (小雪)	$P(\lambda_S + 2\pi/3)$
J11 (大雪)	$P(\lambda_S + 7\pi/12)$	Z11 (冬至)	$P(\lambda_S + \pi/2)$
J12 (小寒)	$P(\lambda_S + 5\pi/12)$	Z12 (大寒)	$P(\lambda_S + \pi/3)$

Note that the moon phase calculation only involves the *difference* $\lambda_M - \lambda_S$. This is the angular distance between the Moon and Sun projected onto the ecliptic. Therefore, it has nothing to do with nutation, which describes the wobble of Earth's spin axis. We can thus simplify the calculation by setting the nutation in longitude $\Delta\psi = 0$ in the computation of $\lambda_M - \lambda_S$. Mathmatically speaking, the matrix $\mathbf{R}_3(-\Delta\psi)$ in $\mathbf{R}_1(\epsilon)\mathbf{N}$ adds the angle $\Delta\psi$ to the ecliptic longitude. Since the same angle is added to λ_M and λ_S , $\lambda_M - \lambda_S$ is independent of $\Delta\psi$, and I have verified numerically that this is indeed the case. From the physical consideration it is also apparent that only precession of the ecliptic affects $\lambda_M - \lambda_S$. The dominant component of the precession, the precession of the equator, must be cancelled in a similar way as the nutation term (see Section 7.3 below). However, I don't try to simplify the precession calculation because it is computationally inexpensive.

7.1 Newton-Raphson Method

In our case, the best method for finding the roots of $f(t) = 0$ is the Newton-Raphson method. This is an iterative scheme. Suppose t_n is the approximate value of a root in the n th iteration. The improved approximation in the $(n + 1)$ th iteration is given by the equation

$$t_{n+1} = t_n - \frac{f(t_n)}{\dot{f}(t_n)} \quad (47)$$

This scheme requires the time derivative of f , which is $\dot{\lambda}_S$ for 24 solar terms and $\dot{\lambda}_M - \dot{\lambda}_S$ for moon phases. They can be computed using the method described in the previous section. An initial guess is required to start the iteration. This turns out to be very easy. We know that the motion of the Sun and Moon are fairly uniform because of the low eccentricity of the Earth's orbit around the Sun and the low eccentricity of the Moon's orbit around the Earth. As a result, both $\dot{\lambda}_S$ and $\dot{\lambda}_M$ do not change significantly and can be used to calculate the approximate time when λ_S or $\lambda_M - \lambda_S$ reaches a certain value. Suppose we want to find a root of $f(t) = 0$ close to a

given TDB time t_0 . We can simply set $t_1 = t_0 - f(t_0)/\dot{f}(t_0)$. However, it is an approximation to a root since we know $f(t) = 0$ has multiple roots in our cases. Sometimes we may want to find a specific root, e.g. the first new moon before a particular winter solstice or the first full moon after a particular new moon. In cases like these, we want to find the first root before or after a given TDB time t_0 . We can modify the initial guess t_1 according to the following equation:

$$t_1 = t_0 - \frac{f(t_0)}{\dot{f}(t_0)} + \frac{2k\pi}{\dot{f}(t_0)}, \quad (48)$$

where k is an integer that takes the value of 0, 1 or -1 . As mentioned above, \dot{f} is close to being a constant. In the case of 24 solar terms, $2\pi/\dot{f}$ is close to a tropical year (365.2422 days). In the case of moon phases, $2\pi/\dot{f}$ is close to a synodic month (29.5306 days). Hence, the addition of $2k\pi/\dot{f}(t_0)$ is just to add/subtract a period to the original guess $t_0 - f(t_0)/\dot{f}(t_0)$. It works as follows.

Case 1: Want to find the first root *before* t_0 . In this case, we want $t_1 < t_0$. Hence if $f(t_0) > 0$ set $k = 0$; if $f(t_0) < 0$ set $k = -1$. (Note that $f(t_0) \in [-\pi, \pi)$ and $\dot{f}(t_0) > 0$ for both moon phases and 24 solar terms.)

Case 2: Want to find the first root *after* t_0 . In this case, we want $t_1 > t_0$. Hence if $f(t_0) > 0$ set $k = 1$; if $f(t_0) < 0$ set $k = 0$.

Once t_1 is determined, the iteration procedure can be started. The sequence $\{t_n\}$ converges very rapidly. I stop the process at iteration m when $|t_m - t_{m-1}| < \varepsilon$ and I set $\varepsilon = 10^{-8}$ days = 0.864 milliseconds. It follows from equation (47) that this convergence criterion is equivalent to setting $|f(t_{m-1})/\dot{f}(t_{m-1})| < \varepsilon$. Note that 10^{-8} days are close to the floating-point round-off precision. Project Pluto's C code takes the Julian date number JD as an input for computing the positions and velocities. The JD of J2000.0 is 2451545. This is a 7-digit integer. In fact, the integer part of the JD from 1976 BCE to 22666 CE are all 7-digit integers. A precision of 10^{-8} days means the JD is accurate to 15 significant figures.

Newton-Raphson method turns out to be very effective in the computation of the times of moon phases and 24 solar terms. After setting t_1 , the method converges to the required accuracy within 3 or 4 iterations. As a result, it only takes about 17 seconds to compute all the times of the 4 moon phases and all 24 solar terms from years 1600 to 3500 using my somewhat old computer at home.⁵ In the early development of my code, I didn't use equation (31) to simplify the calculation of the matrix $\mathbf{R}_1(\epsilon)\mathbf{N}$ and computed the unnecessary quantity $\Delta\epsilon$ and also calculated the unnecessary quantity $\Delta\psi$ in the moon phase calculation. It took about 90 seconds to do the same calculation. The series involving $\Delta\epsilon$ contains 1056 terms involving trigonometric functions. The series involving $\Delta\psi$ contains 1358 terms of trigonometric functions. When I only kept a few terms in $\Delta\psi$ and $\Delta\epsilon$, the computation finished in a few seconds. From this information I conclude that most of the computation time is spent in computing $\Delta\psi$. This is probably not true if I had used a semi-analytic ephemeris such as VSOP87 or ELP/MPP02, which involves Poisson series containing thousands of terms involving trigonometric functions. This is the advantage of using the JPL ephemerides since the positions and velocities are simply computed by interpolation of the tabulated values using

⁵Update in June 2021: The old computer has been retired. The same calculation (all moon phases and solar terms from 1600 to 3500) now takes only about 6 seconds in my new computer. However, the code is compiled using a newer C++ compiler and is executed in a different Linux distribution. The substantial speedup is likely caused by improvement in both hardware and software.

the Chebyshev polynomials and their derivatives. The computation is much faster and the result is more accurate than other semi-analytic theories. One disadvantage of the JPL ephemerides is that they require large data files in order for the accuracy of the interpolated data to match the accuracy of the numerical integration. However, even the largest data files (for DE431 and DE441) are about 2.6GB, which is not much in today's computation world. Another disadvantage is that it is not possible to extrapolate to times beyond the time span covered by the ephemerides. For DE431 and DE441, the time span is from years -13,200 to 17,191, which should be adequate for many applications.

As mentioned above, my criterion for convergence is equivalent to setting $|f(t)/\dot{f}(t)| < \varepsilon$. Hence the accuracy is mainly determined by how close $f(t)$ is towards 0. The role of \dot{f} is to provide a conversion factor between the deviation of $|f(t)|$ from 0 to the error in the computed time. I mention in the previous sections that there is some error in the computation of \dot{f} because I drop some terms. In particular, dropping the factor dt_r/dt in equation (38) introduces a fractional error of $\sim 10^{-6}$ for the Sun and $\sim 10^{-7}$ for the Moon. Dropping the second term in equation (44) introduces a fractional error of $\sim 4 \times 10^{-5}$ for the Sun and $\sim 3 \times 10^{-6}$ for the Moon. Since the accuracy is set by $|f(t)/\dot{f}(t)| < \varepsilon$, error in \dot{f} is equivalent to changing ε . Thus, a fractional error of 10^{-4} is the same as changing ε to 1.0001ε in the worse cases. For $\varepsilon = 10^{-8}$ days = 0.864 ms, that is the difference between 0.864 ms and 0.8640864 ms. Therefore, the accuracy of the computed times is almost independent of the small error in \dot{f} . Even a 10% error in \dot{f} is harmless as long as ε is set to a much smaller value than the target accuracy. Since I know \dot{f} is nearly constant, I tried setting it to its average value just out of curiosity. So I tried $\dot{f} = 2\pi/29.5306\text{days}$ for the moon phase calculation and $\dot{f} = 2\pi/365.2422\text{days}$ for the solar term calculation. When compared to the calculation using accurate \dot{f} , I find a maximum deviation of 0.16 ms for the 24 solar terms and 0.24 ms for moon phases from years 1600 to 3500. These are all smaller than the prescribed ε . However, this does not mean that accurate values of \dot{f} are useless because even though the accuracy does not suffer, the number of iterations required to reach convergence increases. Using these inaccurate values of \dot{f} takes up to 7 iterations for the solar term calculation to converge to the required accuracy, and up to 12 iterations for the moon phase calculation to converge, causing a significant slowdown in the calculation. It is well-known that Newton-Raphson method is a second-order scheme, which converges much faster than first-order root-searching schemes. However, it is only second order if the derivative is accurate. Computing \dot{f} using JPL ephemerides is very straightforward. \dot{f} involves velocities of the Earth, Moon and Sun. In the published ephemerides, velocities are computed by taking the time derivative of the positions. Since positions are expressed as a sum over Chebyshev polynomials, the time derivative involves the first derivatives of the Chebyshev polynomials. Both Chebyshev polynomials and their derivatives are simply computed using recurrence equations.

7.2 Comparison with Different Ephemerides and with a Different Precession Model

I have computed the TDB times of the moon phases and 24 solar terms using JPL's DE431 and DE430. As mentioned above, the only difference between DE430 and DE431 is that DE430 includes a core/mantle damping term in calculating the position of the Moon. JPL recommends using DE430 for times within few hundred years from J2000.0 and DE431 for earlier and later periods. Comparing the computed times of moon phases and 24 solar terms between DE430 and DE431, I find a maximum difference of 0.000419 s ($< \varepsilon$) in 24 solar terms and 0.85 s in moon phases between years 1600 and 2500. Note that the maximum deviations in the times of 24 solar

terms are less than the prescribed convergence criterion $\varepsilon = 0.000864$ s and so there is essentially no difference in the times of 24 solar terms.

DE405 was released in 1998 and was the basis for the Astronomical Almanac from 2003–2014. DE406 was released at the same time as DE405. The integration method used in DE406 was the same as that of DE405, but the accuracy of the interpolating polynomials has been lessened to reduce file size for the longer time span covered by the file. Comparing the computed times of moon phases and 24 solar terms between DE406 and DE431, I find maximum deviations of 0.14 s in 24 solar terms and 0.18 s in moon phases for years between 1600 and 2500.

DE440 and DE441 were released in 2020. Comparing the times of the moon phases and 24 solar terms between DE440 and DE431, I find maximum deviations of 0.81 seconds in 24 solar terms and 1.06 seconds in moon phases for years between 1600 and 2500. The maximum deviations reduce to 0.15 seconds for solar terms and 0.08 seconds for moon phases when years from 1800 and 2200 are compared. For DE431 and DE441, the maximum deviations are 0.81 seconds for solar-term times and 1.15 seconds for moon-phase times for years between 1600 and 2500. The deviations are reduced to 0.15 seconds for solar-term times and 0.11 seconds for moon-phase times for years between 1800 and 2200.

As pointed out in [Vondrák et al 2011], the IAU 2006 precession model is only accurate within about 1000 years from J2000.0. In the paper the authors developed a new precession model that can be used within 200 millennia from J2000.0. This precession model is adopted by the popular open-source planetarium software Stellarium. I also use it for my star chart website. As mentioned above, in 2020 JPL adopted this precession model to replace the older Lieske (1979) precession model for Earth’s orientation in their numerical integration to generate the DE440 and DE441 ephemerides.

In my implementation of the [Vondrák et al 2011] precession model, the angles ψ_A , ω_A and χ_A in equation (18) are replaced by equations (11), (13), Tables 4 and 6 in [Vondrák et al 2011]. Comparing the times of moon phases and 24 solar terms computed by DE431 with the new precession model and by DE431 with the IAU 2006 precession model, I find maximum deviations of 0.19 s in 24 solar terms and 0.00037 s ($< \varepsilon$) in moon phases for years between 1600 and 2500, but the maximum deviations go up to 3 s in 24 solar terms and 0.0035 s in moon phases when comparing the times for years from 1600 to 3500. The big difference between the deviation in the times of solar terms and moon phases is not surprising. The 24 solar terms are defined by the apparent longitude of the Sun, which is the angle measured from the true vernal equinox to the position of the Sun along the true equator; whereas moon phases are defined by the *difference in longitude* of the Moon and Sun, which is the angular separation between the Moon and Sun projected onto the ecliptic. The moon phases are thus affected only by the precession of the ecliptic, which is much smaller than the precession of the equator. The 24 solar terms are affected by both the precession of the equator and precession of the ecliptic. The Moon’s apparent motion in the sky is also much faster than the Sun’s apparent motion. All these make the deviation in the times of moon phases much smaller than those of the solar terms.

Based on these comparisons, I estimate that the TDB times of the computed moon phases and 24 solar terms using DE431 and IAU 2006 precession model are probably accurate to better than 0.2 s for years between 1800 and 2200.

DE441 and DE431 cover the same time span, so it’s possible to make comparisons over a longer period of time. By comparing years between -2000 and 2500, I find that the maximum deviation of the TDB solar-term times is 45 seconds, occurring in -2000. The maximum deviation of the TDB moon-phase time is 416 seconds, occurring in -1999. This shows a more substantial deviation between DE431 and DE441 in the distant past. However, it is the UT1 that is relevant to calendar

making and eclipse calculation. Unfortunately, we don't have accurate data for the conversion between TDB and UT1 before 1600. The uncertainty of $\Delta T = TT - UT1 \approx TDB - UT1$ around -2000 is estimated to be about 0.3 hours (see the Earth Rotation page by the HM Nautical Almanac Office), which is larger than the TDB time differences of moon phases and solar terms between DE441 and DE431.

7.3 Fukushima-Williams Parameterization of Precession

The IAU 2006 precession matrix in equation (16) adopts the Capitane, Wallace, and Chapront parameterization. There are other representations of precession (see [Urban & Seidelmann 2013], Section 6.6.2). One particular representation that's worth mentioning is the Fukushima-Williams parametrization:

$$\mathbf{P} = \mathbf{R}_1(-\epsilon_A)\mathbf{R}_3(-\Psi)\mathbf{R}_1(\phi)\mathbf{R}_3(\gamma). \quad (49)$$

Let \mathcal{C}_0 be the ecliptic north pole at J2000.0, \mathcal{C} be the ecliptic north pole of date, \mathcal{P}_0 be the mean celestial north pole at J2000.0, and \mathcal{P} be the mean celestial north pole of date. The angle γ is the angle between \mathcal{C}_0 and \mathcal{C} viewed from \mathcal{P}_0 ; ϕ is the arc from \mathcal{P}_0 to \mathcal{C} ; Ψ is the angle from \mathcal{P}_0 to \mathcal{P} viewed from \mathcal{C} ; ϵ_A is the mean obliquity of the ecliptic of date. Figure 6.4 of [Urban & Seidelmann 2013] depicts these angles. Another way to describe ϕ is that it's the inclination angle between the ecliptic of date and the mean equator of J2000.0. The angle γ is the difference between the right ascension of \mathcal{C} and the right ascension of \mathcal{C}_0 (which is $-\pi/2$) with respect to the mean equator and equinox of J2000.0. The angle Ψ is the difference between the ecliptic longitude of \mathcal{P} (which is $\pi/2$) and the ecliptic longitude of \mathcal{P}_0 with respect to the ecliptic and mean equinox of date. It is apparent that γ and ϕ are related to the precession of the ecliptic and Ψ is related to the precession of the equator viewed from the ecliptic pole of date. Combining equation (31) and (49) yields

$$\mathbf{R}_1(\epsilon)\mathbf{N}\mathbf{P} = \mathbf{R}_3(-\Delta\Psi)\mathbf{R}_3(-\Psi)\mathbf{R}_1(\phi)\mathbf{R}_3(\gamma) = \mathbf{R}_3(-\Delta\Psi - \Psi)\mathbf{R}_1(\phi)\mathbf{R}_3(\gamma). \quad (50)$$

The matrix $\mathbf{R}_3(-\Delta\Psi - \Psi)$ adds an angle $\Psi + \Delta\Psi$ to the ecliptic longitude. The addition is cancelled in $\lambda_M - \lambda_S$ and so we don't need to include $\mathbf{R}_3(-\Delta\Psi - \Psi)$ in the moon phase calculation. It's now apparent that the times of moon phases are only affected by the precession of the ecliptic.

For the precession model compatible with the IAU 2006 model, the angles γ , ϕ and Ψ can be calculated using the expressions in Table 6.3 of [Urban & Seidelmann 2013]:

$$\begin{aligned} \gamma &= 10.556403''T + 0.4932044''T^2 - 0.00031238''T^3 \\ &\quad - 2.788'' \times 10^{-6}T^4 + 2.60'' \times 10^{-8}T^5 \\ \phi &= 84381.406'' - 46.811015''T + 0.0511269''T^2 + 0.00053289''T^3 \\ &\quad - 4.40'' \times 10^{-7}T^4 - 1.76'' \times 10^{-8}T^5 \\ \Psi &= 5038.481507''T + 1.5584176''T^2 - 0.00018522''T^3 \\ &\quad - 2.6452'' \times 10^{-5}T^4 - 1.48'' \times 10^{-8}T^5 \end{aligned} \quad (51)$$

While equation (50) together with (51) will not give an numerically identical matrix as that computed using the IAU 2006/2000A precession-nutation model (i.e. the matrix computed using equations (16), (18) and (31)), the result is the same within the accuracy of the IAU 2006 precession model. I have compared the times of moon phases and solar terms computed by (50) and (51) with those computed using the IAU 2006/2000A precession-nutation theory (both using DE 431 for the positions of the Sun and Moon). I find that in the years from 1600 to 2500, the time

differences are no more than 0.00016 seconds ($< \epsilon$) for the solar terms and moon phases. While mathematically more elegant, equation (50) doesn't significantly speed up the overall computation, which is expected since the precession calculation is computationally inexpensive.

7.4 Text Files for the TDB Times

Even though the computation of the TDB times of moon phases and 24 solar terms is complicated, it only needs to be done once for a given ephemeris and precession-nutation model. I use DE431 to calculate the times mainly because of its long time span (-13200–17191). Even though DE441 replaced DE431 in 2020, the TDB time differences of moon phases and 24 solar terms between these two ephemerides are insignificant in recent centuries. For the distant past and distant future, the TDB time differences are smaller than the uncertainty of ΔT as mentioned before. Therefore, DE441 does not produce more accurate UT1+8/UTC+8 times than DE431. At this moment, there is no compelling reason for me to update the data for the Chinese Calendar website.

I created two text files in ASCII format storing these times computed from DE431. The first file is `TDBtimes.txt`, covering years from 1600 to 3500. The second file is `TDBtimes_extended.txt`, covering years from -4000 to 8000. These two files are available on my GitHub repository in the `src` directory. The second file is compressed to reduce the size. It is listed as `TDBtimes_extended.txt.gz` in the repository. It can be decompressed using Linux's `gzip` or other similar programs.

Times in `TDBtimes.txt` are computed using the IAU2006/2000A precession-nutation model. As mentioned above, the IAU2006 precession model is only accurate within about 1000 years from J2000.0. Times in `TDBtimes_extended.txt` are computed using the precession model of [Vondrák et al 2011], which is valid within 200 millennia from J2000.0. It is not clear what the time span of validity of the IAU2000A nutation model is. The lunar and solar arguments in (21) used by the nutation model are taken from [Simon et al 1994] and the authors in the paper recommended the optimal use between 4000 BC and 8000 AD. I assume that this is probably about the time span of validity of the IAU2000A nutation model. That is why `TDBtimes_extended.txt` covers years from -4000 (4001 BC) to 8000.

These two files are designed for use in the calculation of Chinese calendar. I will focus on the file `TDBtimes.txt` first and then mention an important note when using the data in `TDBtimes_extended.txt`.

The file `TDBtimes.txt` contains 1901 rows and 87 columns. The first column is the Gregorian year. The second column, named `jd0`, is the Julian date number on January -1 of the year at 16:00 TDB, or January 0 of the year at 0:00 (TDB+8). For example, the `jd0` in the year 2000 is 2451543.166666667. This was the Julian date number on January -1, 2000 at 16:00 TDB (December 30, 1999 at 16:00 TDB). The value of `jd0` is always an integer plus 1/6 because the TDB time is always 16:00. `jd0` is the time origin from which the times in the rest of the columns are measured. That is, the Julian date numbers of the times in the rest of the columns are `jd0 + values` listed in those columns.

The third column, labelled `Z11a`, is the time of the winter solstice *closest to* `jd0`. For the time span in the file, `Z11a` is the time of the December solstice in the previous year. For example, the third column in year 2000 is `-8.343841734507215`. This means that the December solstice in 1999 occurred at TDB Julian day `2451543.166666667 - 8.343841734507215`, which was December 22, 1999 at 7:44:52 TDB. Columns 4–27 are the 24 solar terms following `Z11a`, starting from `J12` (小寒) and ending with `Z11` (labelled `Z11b`). The time listed in column `Z11b` is the same as the time listed in `Z11a` in the following year. Their values are different simply because they are measured from different time origins.

Column 28, labelled Q0_01, is the time of the first new moon occurring *before* the winter solstice listed in the Z11a column. The remaining columns (Columns 29–87) are the times of the first quarters (labelled Q1_xx), full moons (labelled Q2_xx), third quarters (labelled Q3_xx) and other new moons (labelled Q0_xx) in chronological order. Here xx ranges from 01 to 15 representing the lunation number counting from the new moon in column 28. Each year lists the four moon phases covering 15 lunations.

The data structure in `TDBtimes_extended.txt` is the same as that in `TDBtimes.txt`. Following the usual convention, Julian calendar is used before October 15, 1582. Thus, the `jd0` before 1583 refers to the Julian date number on January -1 of the year at 16:00 TDB in the Julian calendar. The date following October 4, 1582 was October 15, 1582 because of the Gregorian reform, although not all countries adopted the Gregorian calendar on this day. This explains why the difference in `jd0` between 1582 and 1583 is only 355 days. Since the average Julian year is 365.25 and is slightly longer than the tropical year, before 1583 the average time of the winter solstice, as well as all the other 24 solar terms, drifted one day earlier every 128 years in the Julian calendar. For years before -1128, winter solstices could occur in January in the Julian calendar.

The data structure of these two files is designed for convenience in the computation of the Chinese calendar in the *suì* from the winter solstice Z11a to the winter solstice Z11b. The new moon listed in the Q0_01 column is usually but not always associated with month 11 in the Chinese calendar. Even though by definition the new moon in the Q0_02 column must occur after the winter solstice, it could happen that it is on the same day as the winter solstice if it occurs only a few hours later than the winter solstice. If that is the case, it is the new moon in the Q0_02 column that is associated with month 11. To determine if this is the case requires the knowledge of the beginning and ending of a day. The Chinese calendar uses UTC+8 to define a day, so we will need to know the conversion between TDB and UTC to determine accurately if that is the case. A *suì* can contain up to 13 Chinese months, which requires 14 new moons to determine the number of days in each of the 13 months. If month 11 starts on the date of the second new moon, it must be on the same day as the winter solstice. It is easy to show that the *suì* can only have 12 months in that case. So in all cases 14 new moons are sufficient to determine all months in a *suì*. Listing moon phases covering 15 lunations is more than enough for the calendar calculation, and there are some overlaps between the moon phases listed in a year and those listed in the previous and the following year.

8 Conversion Between TDB and UTC

The choice of separating the computation of times in TDB and conversion between TDB and UTC is deliberate. The computation of the TDB times is complicated but only need to be done once for any given ephemeris and precession-nutation model. The conversion between TDB and UTC is constantly modified as new data become available. By separating the two procedures, each time the conversion between TDB and UTC is modified, we just need to update the conversion and do not need to recompute the times of moon phases and 24 solar terms. If the UTC+8 times were given in the text files `TDBtimes.txt` and `TDBtimes_extended.txt`, they would become outdated when a modified conversion emerges.

UTC was invented in 1960. There were several changes in UTC until it was finalized in 1972. To prevent confusion, I use UT1+8 for times before 1972. Conversion between TDB and TT is ignored because the deviations between the two times are less than 0.002 s over several millennia. For years before 1972, values of $\Delta T = \text{TT} - \text{UT1}$ are calculated using the fit-

ting and extrapolation formula by [Stephenson et al 2016] and [Morrison et al 2021] (see also the HMNAO Earth rotation webpage for a summary). UT1 is obtained by simply subtracting ΔT from TDB. For years from 1972 to the present day, I use a table of published leap seconds (e.g. https://en.wikipedia.org/wiki/Leap_second) to calculate $TT - UTC$. Specifically,

$$\begin{aligned} TT - UTC &= (TT - TAI) + (TAI - UTC) \\ &= 42.184 \text{ s} + \text{total number of leap seconds added to UTC since 1972.} \end{aligned} \quad (52)$$

For the future years, I use the extrapolation formula for ΔT derived from [Stephenson et al 2016] and [Morrison et al 2021] to estimate $TT - UTC$. Specifically, the extrapolation formula is obtained by integrating their long-term lod function:

$$\begin{aligned} t &= (y - 1825)/100 \quad , \quad f(y) = 31.4115t^2 + 284.8436 \cos[2\pi(t + 0.75)/14], \\ \Delta T &= c_2 + f(y), \end{aligned} \quad (53)$$

where y is year, t is the number of centuries from 1825, and $c_2 = -150.315$. The formula gives ΔT in seconds. The value of c_2 is chosen to make ΔT continuous at $y = 2022$. For a given Julian date number JD , y may be calculated by $y = (JD - 2451544.5)/365.2425 + 2000$. By construction, $|UTC - UT1| < 0.9 \text{ s}$, so the error in setting $TT - UTC$ to ΔT is probably less than the error in the extrapolation formula.

These fitting and extrapolation formulae are used on my eclipse website. I have also created a GitHub repository to provide python functions to calculate ΔT and to provide error estimates.

In the following I give two examples to demonstrate how the conversion works.

Example 1: From the text file `TDBtimes.txt`, the first new moon in the year 2018 is the new moon in the `Q0_02` column (column 32). The TDB time of the new moon is 17.42943724648089 days from January 0, 2018 at 00:00 (TDB+8), which is January 17, 2018 at 10:18:23.378 (TDB+8). According to the leap second table, the total number of leap seconds added to UTC in 2018 is 27 s. Hence $TT - UTC = 69.184 \text{ s}$. Subtracting 69.184 s from the TDB+8 time above, I find the new moon occurred on January 17, 2018 at 10:17:14 (UTC+8). This is consistent with the time listed in *Astronomical Phenomena for the year 2018* (January 17, 2018 at 02:17 UTC) published jointly by The Nautical Almanac Office and Her Majesty's Nautical Almanac Office. This is not surprising since the astronomical data of the book are based on DE430 and the time differences of the moon phases calculated by DE431 and DE430 are no more than 0.2 s in the period 1600–2200 as mentioned in the previous section.

Example 2: From the text file `TDBtimes.txt`, the new moon listed in the column `Q0_13` in year 2165 is 338.0018578149057 days from January 0, 2057 at 00:00 (TDB+8), which is December 4, 2165 at 00:02:40.5 (TDB+8). Using the extrapolation formula (53), I find $\Delta T = 131.8 \text{ s}$. Setting $TT - UTC \approx 131.8 \text{ s}$ and subtracting it from the TDB+8 time above gives the new moon occurring on December 4, 2165 at 00:00:29 (UTC+8). This is just 29 s past midnight! If the extrapolation value is smaller than the actual value by more than 29 s, this new moon will fall on December 3, 2165. This new moon is associated with month 11 in the Chinese calendar. Therefore, it is currently not possible to determine the exact start day of month 11 in 2165. We just have to wait for the time to come to get a better handle on the situation.

As we see, the conversion between TDB and UTC depends on the number of leap seconds added to UTC. It is very difficult, if not impossible, to predict accurately how many leap seconds will be added to UTC decades from now because of the irregularity of Earth's rotation. The situation may also be complicated by the uncertainty of the leap-second policy in the future: there have been discussions on the abolishment of leap seconds since 2005.

References

- [Capitaine et al 2003] N. Capitaine, P.T. Wallace, and J. Chapront, “Expressions for IAU 2000 precession quantities”, *Astron. Astrophys.*, 412(2), pp. 567-586, 2003, doi:10.1051/0004-6361:20031539.
- [Folkner et al 2014] W.M. Folkner et al, “The Planetary and Lunar Ephemerides DE430 and DE431”, IPN Progress Report 42-196, February 15, 2014.
- [GB/T 33661-2017] 《农历的编算和颁行》 (“Calculation and promulgation of the Chinese calendar”), revised version (June 28, 2017), issued jointly by General Administration of Quality Supervision, Inspection and Quarantine of the People’s Republic of China and Standardization Administration of the People’s Republic of China, drafted by Purple Mountain Observatory.
“国家标准《农历的编算和颁行》解读材料” (“Explanatory material for ‘Calculation and promulgation of the Chinese calendar’ ”), Purple Mountain Observatory, Chinese Academy of Science.
- [IERS Conventions 2010] IERS Conventions 2010, edited by G. Petit and B. Luzum.
- [Kaplan 2005] G.H. Kaplan, “The IAU Resolutions on Astronomical Reference Systems, Time Scales, and Earth Rotation Models: Explanation and Implementation”, U.S. Naval Observatory Circular No. 179, U.S. Naval Observatory, Washington, D.C. 20392 (2005).
- [Morrison et al 2021] L.V. Morrison, F.R. Stephenson, C.Y. Hohenkerk, and M. Zawilski, “Addendum 2020 to ‘Measurement of the Earth’ s rotation: 720 BC to AD 2015’ ”, *Proc. R. Soc. A.*, 477:20200776 (2021).
- [Newhall 1989] X.X. Newhall, “Numerical Representation of Planetary Ephemerides”, *Celestial Mechanics and Dynamical Astronomy*, Vol. 45, p.305, 1989.
- [Park et al 2021] R.S. Park et al, “The JPL Planetary and Lunar Ephemerides DE440 and DE441”, *The Astronomical Journal*, 161, 105, 2021.
- [Simon et al 1994] J.L. Simon et al, Numerical expressions for precession formulae and mean elements for the Moon and the planets, *Astron. Astrophys.*, 282, 663 (1994).
- [Stephenson et al 2016] F.R. Stephenson, L.V. Morrison, and C.Y. Hohenkerk, “Measurement of the Earth’s rotation: 720 BC to AD 2015”, *Proc. R. Soc. A.*, 472:20160404 (2016).
- [Titov, Lambert & Gontier 2011] O. Titov, S.B. Lambert and A.-M. Gontier, VLBI measurement of the secular aberration drift, *Astron. Astrophys.*, 529, A91 (2011).
- [Urban & Seidelmann 2013] S.E. Urban and P.K. Seidelmann, *Explanatory Supplement to the Astronomical Almanac*, 3rd edition, University Science Books, Mill Valley, California (2013). Errata:
https://aa.usno.navy.mil/downloads/exp_supp_errata.pdf

[Vondrák et al 2011]

J. Vondrák, N. Capitaine, and P. Wallace, “New precession expressions, valid for long time intervals”, *Astron. Astrophys.*, 534, A22 (2011).

Appendix

The calculations in this appendix are hardly relevant to the calculation of moon phases and 24 solar terms. They are included here because the results are mentioned in Section 5 and the topics are interesting by themselves.

A Position and Velocity of the Sun

As mentioned in Section 5, the Sun contains 99.86% of all masses in the solar system. As a result, the Sun barely moves with respect to the solar system barycenter (SSB). One can first estimate the amount of movement of the Sun before doing a full calculation.

Apart from the Sun, the most massive object in the solar system is Jupiter. The mass of Jupiter is $M_J = M_\odot/1047$, where M_\odot is the solar mass. Jupiter’s orbit is slightly eccentric (orbital eccentricity ≈ 0.05) with a semi-major axis of $a_J = 5.2 \text{ AU} = 1120R_\odot$, where $R_\odot = 6.957 \times 10^5 \text{ km}$ is the solar radius. The orbital period of Jupiter is $P_J = 4332.6 \text{ days}$. Jupiter’s gravity alone will make the Sun move in a slightly eccentric orbit with a semi-major axis $a_\odot = (M_J/M_\odot)a_J = 1.07R_\odot$ and with an orbital speed of $v_\odot \approx 2\pi a_\odot/P_J = 12.5 \text{ m/s}$.

Let’s now look at the actual motion of the Sun with respect to the SSB. This can be calculated directly from JPL’s ephemerides. The following shows the calculation using DE431. Figures 1 and 2 show the barycentric trajectory of the Sun from 1950 to 2050 in the ecliptic coordinate system associated with the ecliptic and mean equinox of J2000.0. To be precise, the vector $\mathbf{X}_{\text{ec2000}} = (X_{\text{ec2000}} \ Y_{\text{ec2000}} \ Z_{\text{ec2000}})^T$ is calculated by

$$\mathbf{X}_{\text{ec2000}} = \mathbf{R}_1(\epsilon_0)\mathbf{B}\mathbf{x}, \quad (54)$$

where \mathbf{x} is the Sun’s BCRS coordinates, \mathbf{B} is the frame bias matrix (11), \mathbf{R}_1 is the rotation matrix (14), and $\epsilon_0 = 84381.406''$ is the inclination angle between the ecliptic and mean equator at J2000.0.

The two plots show that the motion of the Sun is more complicated than a slightly eccentric orbit, indicating that gravity from other solar system objects also has significant contribution to the Sun’s motion. Figure 3 shows the speed of the Sun with respect to the SSB. The data indicate that the speed is less than 16.5 m/s with the root mean square value of 12.8 m/s. As a result, the light-time correction shifts the Sun’s position by an amount $v/c < 5.5 \times 10^{-8} \text{ rad} = 0.01''$.

Section 5 also mentions that the radial velocity of the Sun is about 0.5 km/s. This is mainly caused by the eccentricity of Earth’s orbit. The value is estimated by the equation $|v_r| \sim v_{\text{orb}}e$, where $v_{\text{orb}} \approx 30 \text{ km/s}$ is Earth’s orbital speed and $e = 0.0167$ is Earth’s orbital eccentricity. This rough equation can be derived as follows. The radial distance r of a Keplerian orbit is given by the equation

$$r = \frac{a(1 - e^2)}{1 + e \cos \theta}, \quad (55)$$

where a is the orbital semi-major axis and θ is the true anomaly. Differentiating the above equation with respect to time gives

$$v_r = \dot{r} = -\frac{er \sin \theta \dot{\theta}}{1 + e \cos \theta} = -\frac{eh \sin \theta}{r(1 + e \cos \theta)} = -\frac{eh \sin \theta}{a(1 - e^2)}, \quad (56)$$

where $h = r^2 \dot{\theta}$ is the specific angular momentum. From the Newtonian two-body dynamics, we have the following equations:

$$p = a(1 - e^2) = \frac{h^2}{GM} \quad , \quad P^2 = \frac{4\pi^2 a^3}{GM}, \quad (57)$$

where p is called the semi-latus rectum, G is Newton's gravitational constant, M is the total mass of the two-body system and P is the orbital period. The right equation is also known as Kepler's third law (Newtonian version). From the left equation, we can write $h = \sqrt{GMa(1 - e^2)}$ and equation (56) becomes

$$v_r = -e \sqrt{\frac{GM}{a(1 - e^2)}} \sin \theta = -\frac{2\pi a}{P} \frac{e \sin \theta}{\sqrt{1 - e^2}} = -\frac{e \bar{v}_{\text{orb}} \sin \theta}{\sqrt{1 - e^2}}, \quad (58)$$

where $\bar{v}_{\text{orb}} = 2\pi a/P$ is the average orbital speed. Hence, for small eccentricity, $|v_r| \sim e \bar{v}_{\text{orb}}$.

Figure 4 shows the radial velocity of the Sun relative to Earth from 2010 to 2020 calculated using DE431. We see the expected sinusoidal-like variation from the $\sin \theta$ term. Note that θ is nearly but not exactly a linear function of time because of Earth's small eccentricity⁶. The maximum value of $|v_r|$ is 0.515 km/s, very close to the rough estimate.

B Radial Velocity of the Moon

Section 5 mentions that the magnitude of the Moon's radial velocity is $|v_r| \sim 0.05$ km/s. It is estimated again using the rough equation $|v_r| \sim e v_{\text{orb}}$ with $v_{\text{orb}} \approx 2\pi a/P \approx 1$ km/s and $e \approx 0.05$ for Moon's orbital parameters. Figure 5 shows the radial velocity of the Moon calculated using DE431. We see that the radial velocity pattern is more complicated than that of the Sun. The maximum value of $|v_r|$ is 0.074 km/s, which also deviates substantially from the estimated value. These are caused by the perturbations of Moon's orbit by the Sun and other planets. In particular, the Sun's perturbation on Moon's orbit is the greatest. Since the Earth-Moon barycenter is orbiting the Sun, the Sun's perturbation on Moon's orbit arises from the tidal gravity, i.e. the difference between Sun's gravity on the Moon and gravity on the Earth-Moon barycenter. The Sun's tidal gravity on the Moon is about 0.6% of Earth's gravity on the Moon. As the Moon orbits the Earth, it experiences variation of the Sun's tidal gravity as its position relative to the Sun changes, which causes periodic variation of the Moon's orbital parameters. In other words, the Moon's orbital semi-major axis, eccentricity and so on are varying with time.

⁶The true anomaly $\theta(t)$ can be calculated using the standard procedure in celestial mechanics. First calculate the mean anomaly $M(t) = 2\pi(t - T_0)/P$, where T_0 is the time of perihelion passage and P is the orbital period. Next the eccentric anomaly E is determined by solving the Kepler equation $E - e \sin E = M$. Then the true anomaly is calculated by the equation $\tan(\theta/2) = \sqrt{(1+e)/(1-e)} \tan(E/2)$. Note that the mean anomaly $M(t)$ is a linear function of t , but $E(t)$ and $\theta(t)$ are not. Another way to look at it is that the Earth moves with different speeds around the Sun because of its orbital eccentricity. When the Earth is closer to the Sun, it moves faster and so θ increases with a faster rate. When the Earth is farther away from the Sun, it moves slower and so θ increases with a slower rate. As a result, θ is not a linear function of time.

We can visualize the change in Moon's orbital parameters by plotting them versus time. Before I do that, it is useful to understand how the orbital parameters are determined if an object is not moving in a strict Keplerian orbit. The usual approach is to calculate the *osculating orbital elements*, which are Keplerian orbital parameters that give the position and velocity of the object at the given time. The term “osculate” refers to a curve touching (or “kissing”) another curve with the same tangent at the point of contact. The idea is simple. According to the two-body problem of Newtonian mechanics, the relative position and relative velocity of two gravitating bodies are determined by 6 orbital elements $(a, e, i, \omega, \Omega, T_0)$. Here a is the semi-major axis, e is eccentricity, i is the orbital inclination, ω is the argument of periapsis, Ω is the longitude of the ascending node, and T_0 is the time of periapsis passage. The angles i , ω and Ω are three Euler angles specifying the orientation of the orbit with respect to a reference frame; a and e determine the size and shape of the orbit; T_0 specifies a time when the two bodies are closest to each other. Clearly, T_0 is not unique. We can add integer multiples of orbital period P to the values of T_0 . Here P is given by Kepler's third law $P = 2\pi\sqrt{a^3/(GM)}$.

Given these 6 orbital elements, one can calculate the relative position and velocity of the two bodies moving in a Keplerian orbit at any given time. Conversely, knowing the relative position and velocity of the two bodies at a given time, it can be shown that the 5 orbital elements a , e , i , ω and Ω can be determined uniquely provided that $e \neq 0$, $i \neq 0$ and the total mass of the system is known. The element T_0 is determined up to an integer multiples of P . If the two bodies are moving in a strict Keplerian orbit specified by the Newtonian dynamics, the 6 orbital elements determined by the inverse process are time independent (with the exception of T_0 , which is determined up to an integer multiples of P) provided that the coordinate axes of the reference frame from which i , ω and Ω are measured is fixed with respect to the system's barycenter. In the presence of perturbation, one can still use the same equations to calculate the 6 orbital elements from the relative position and velocity, but these orbital elements will change with time. These are the osculating orbital elements. They represent the Keplerian orbit the system would follow if the perturbation were suddenly turned off at the calculation time.

Given the Moon's geocentric position \mathbf{X} and velocity \mathbf{V} at a given time, the osculating semi-major axis a and eccentricity e are very easy to calculate. From the two-body Newtonian dynamics, we have the following equations.

$$\epsilon = -\frac{GM}{2a} = \frac{1}{2}V^2 - \frac{GM}{R} \quad \Rightarrow \quad a = \left(\frac{2}{R} - \frac{V^2}{GM} \right)^{-1}, \quad (59)$$

where ϵ is the specific total orbital energy (total orbital energy per mass) of the system, $R = |\mathbf{X}|$ and $V = |\mathbf{V}|$. This equation can also be obtained directly from the *vis-viva* equation in celestial mechanics. For the Earth-Moon system, $GM = GM_E + GM_M = 8.997011390199871 \times 10^{-10} \text{ AU}^3/\text{day}^2$ using the mass parameters given in Table 8 of [Folkner et al 2014]. The eccentricity is calculated using the equation

$$e = \sqrt{1 + \frac{\epsilon h^2}{(GM)^2}}, \quad (60)$$

where the specific total orbital energy ϵ and specific angular momentum h are calculated using the equations

$$\epsilon = \frac{1}{2}V^2 - \frac{GM}{R}, \quad h^2 = |\mathbf{X} \times \mathbf{V}|^2 = R^2V^2 - (\mathbf{X} \cdot \mathbf{V})^2. \quad (61)$$

Figures 6 and 7 show the Moon's osculating semi-major axis and eccentricity calculated using data from DE431. Data show that there is only a 2% variation in the semi-major axis from the

years 1600 to 3500, but the variation in eccentricity is much larger. The eccentricity varies from 0.0256 to 0.0775 with an average of 0.056. There is a factor of 3 between the maximum and minimum value! This explains why my estimate of maximum $|v_r|$ is off by a factor of 1.5. Of course, this does not affect the conclusion in Section 5: dropping the factor $1/(1 + v_r/c)$ in the calculation of $\dot{\mathbf{X}}_{\text{proper}}$ introduces a negligible error in the computation of $\dot{\lambda}_M$.

C Special Relativistic Aberration of Light

This section derives the special relativistic aberration of light equation (34).

Let \mathbf{p} be the photon 3-momentum in the “lab” frame and \mathbf{p}' be the photon 3-momentum in the moving frame, which moves at 3-velocity \mathbf{v} relative to the “lab” frame. Let $p = \sqrt{\mathbf{p} \cdot \mathbf{p}} = E/c$ be the photon energy/speed of light in the “lab” frame and $p' = \sqrt{\mathbf{p}' \cdot \mathbf{p}'} = E'/c$ be the photon energy/speed of light in the moving frame. Then $\mathbf{n} = -\mathbf{p}/p$ is the unit vector pointing to the direction of the observed photon in the “lab” frame; $\mathbf{n}' = -\mathbf{p}'/p'$ is the unit vector pointing to the direction of the observed photon in the moving frame. Let $\boldsymbol{\beta} = \mathbf{v}/c = \beta \hat{\boldsymbol{\beta}}$. Orient the coordinate system so that the x -axis is in the velocity direction. According to the Lorentz transformation,

$$\begin{pmatrix} p' \\ p'_x \end{pmatrix} = \gamma \begin{pmatrix} 1 & -\beta \\ -\beta & 1 \end{pmatrix} \begin{pmatrix} p \\ p_x \end{pmatrix}, \quad (62)$$

where $\gamma = 1/\sqrt{1 - \beta^2}$, $p_x = \hat{\boldsymbol{\beta}} \cdot \mathbf{p}$, and $p'_x = \hat{\boldsymbol{\beta}} \cdot \mathbf{p}'$. It follows from the p' equation that

$$p' = \gamma(p - \beta p_x) \Rightarrow \frac{p'}{p} = \gamma(1 - \beta p_x/p) = \gamma(1 + \boldsymbol{\beta} \cdot \mathbf{n}). \quad (63)$$

The p'_x equation gives

$$p'_x = \gamma(p_x - \beta p) = -\gamma p(\mathbf{n} \cdot \hat{\boldsymbol{\beta}} + \beta). \quad (64)$$

The components of \mathbf{p}' perpendicular to $\boldsymbol{\beta}$ remain unchanged. Hence

$$\mathbf{p}'_{\perp} = \mathbf{p}_{\perp} = \mathbf{p} - (\mathbf{p} \cdot \hat{\boldsymbol{\beta}})\hat{\boldsymbol{\beta}} = -p[\mathbf{n} - (\mathbf{n} \cdot \hat{\boldsymbol{\beta}})\hat{\boldsymbol{\beta}}]. \quad (65)$$

It follows that

$$\mathbf{p}' = p'_x \hat{\boldsymbol{\beta}} + \mathbf{p}'_{\perp} \quad (66)$$

$$-p' \mathbf{n}' = -\gamma p[(\mathbf{n} \cdot \hat{\boldsymbol{\beta}})\hat{\boldsymbol{\beta}} + \beta] - p[\mathbf{n} - (\mathbf{n} \cdot \hat{\boldsymbol{\beta}})\hat{\boldsymbol{\beta}}] \quad (67)$$

$$\mathbf{n}' = \frac{p}{p'}[\mathbf{n} + \gamma \boldsymbol{\beta} + (\gamma - 1)(\mathbf{n} \cdot \hat{\boldsymbol{\beta}})\hat{\boldsymbol{\beta}}]. \quad (68)$$

Substituting equation (63) into the above equation gives

$$\mathbf{n}' = \frac{\gamma^{-1} \mathbf{n} + \boldsymbol{\beta} + (1 - \gamma^{-1})(\mathbf{n} \cdot \hat{\boldsymbol{\beta}})\hat{\boldsymbol{\beta}}}{1 + \boldsymbol{\beta} \cdot \mathbf{n}}. \quad (69)$$

Since $1 - \gamma^{-1} = 1 - \sqrt{1 - \beta^2} = \beta^2/(1 + \sqrt{1 - \beta^2})$, the above equation can be expressed as

$$\mathbf{n}' = \frac{\gamma^{-1} \mathbf{n} + \boldsymbol{\beta} + (\mathbf{n} \cdot \boldsymbol{\beta})\boldsymbol{\beta}/(1 + \gamma^{-1})}{1 + \boldsymbol{\beta} \cdot \mathbf{n}}, \quad (70)$$

which is equation (34) and is the same as (7.40) in [Urban & Seidelmann 2013]. Note that [Urban & Seidelmann 2013] uses different notations. Their \mathbf{p}_1 is our \mathbf{n}' ; their \mathbf{p} is our \mathbf{n} ; their β is our γ and their \mathbf{V} is our \mathbf{v} .

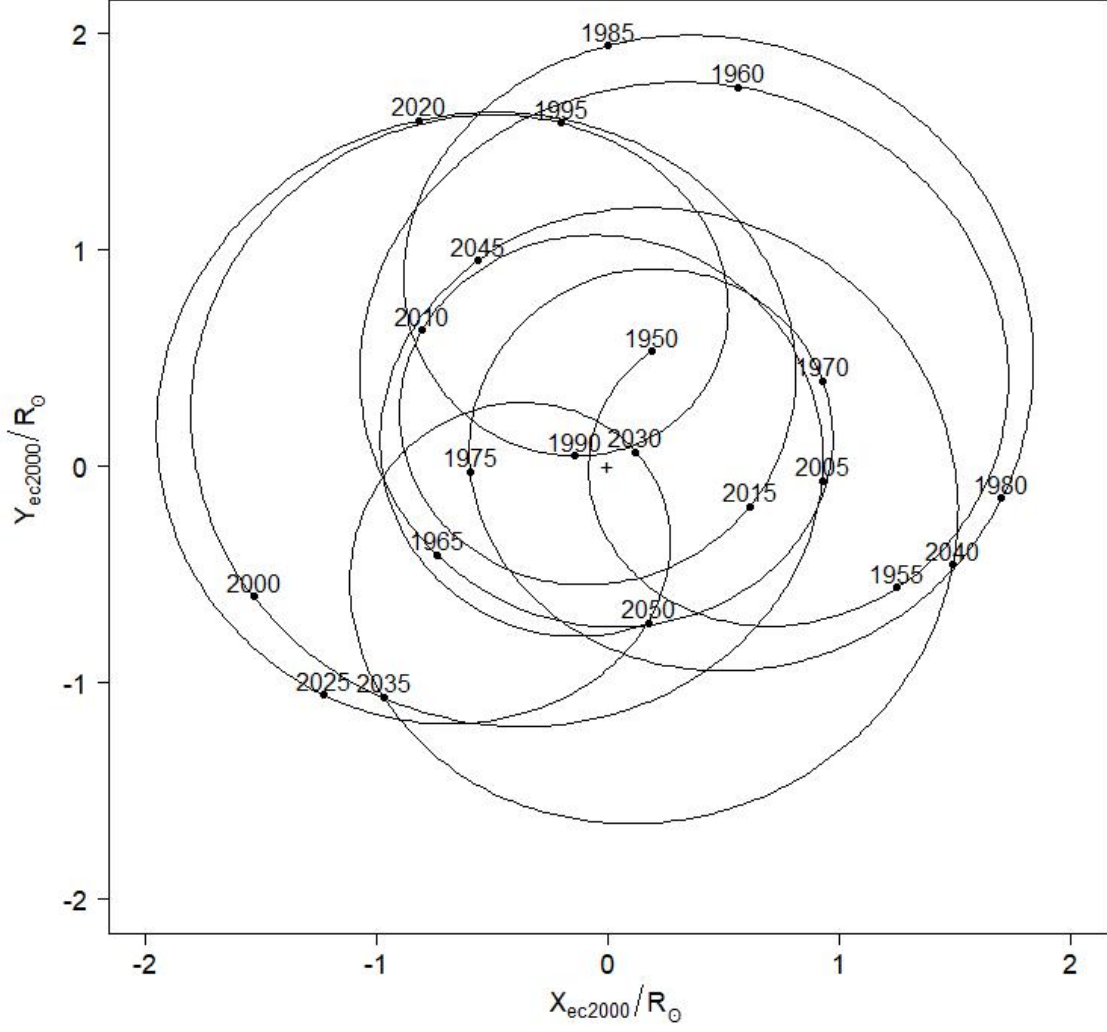


Figure 1: Trajectory of the Sun from 1950 to 2050 in the ecliptic plane of J2000.0. The plus (+) symbol at the center indicates the position of the solar system barycenter (SSB). The numbers indicate the years. The solar radius is $R_{\odot} = 6.957 \times 10^5$ km. The Sun's position is calculated using JPL's DE431 ephemeris.

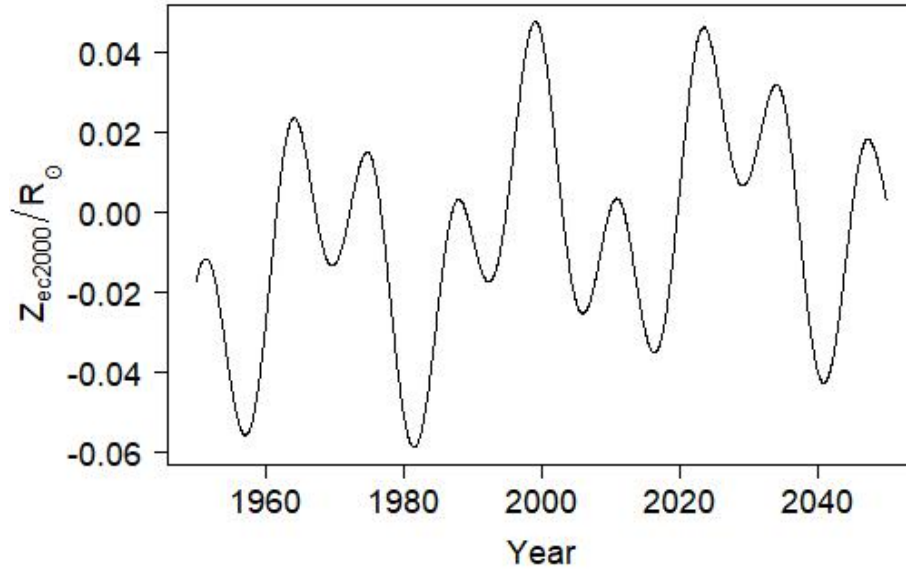


Figure 2: Vertical position of the Sun from the ecliptic of J2000.0. The variable Year is calculated according to $\text{Year} = 2000 + (\text{JD} - 2451544.5)/365.25$, where JD is TDB expressed in Julian date number.

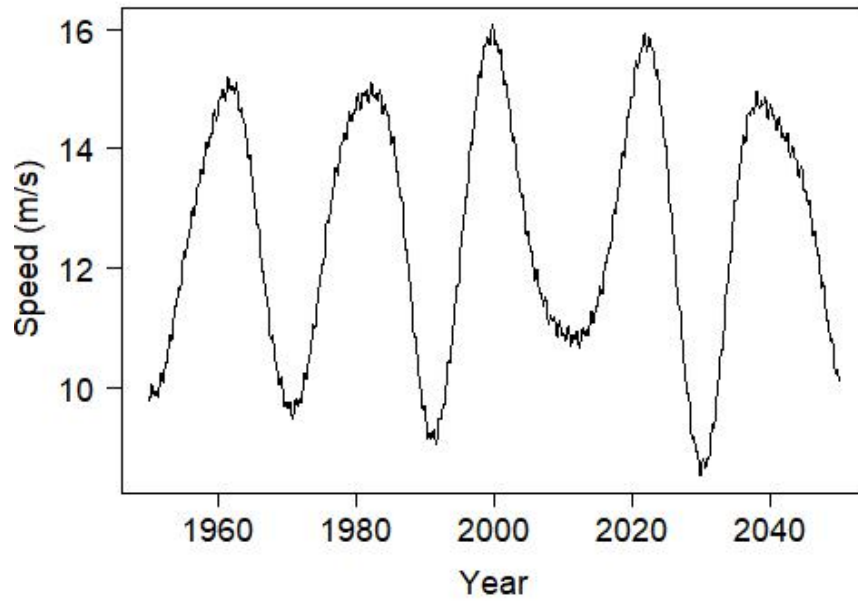


Figure 3: Speed of the Sun with respect to the solar system barycenter.

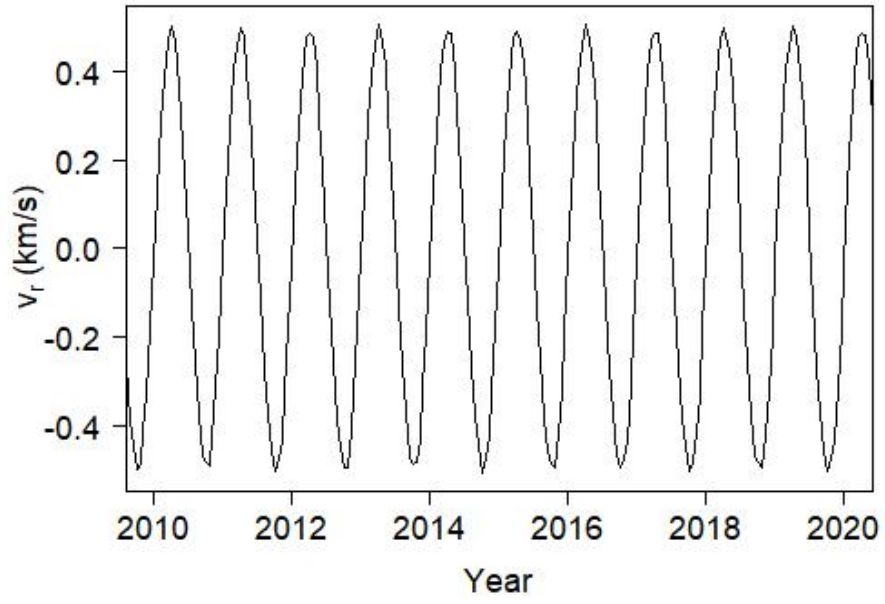


Figure 4: Radial velocity of the Sun relative to Earth from 2010 to 2020.

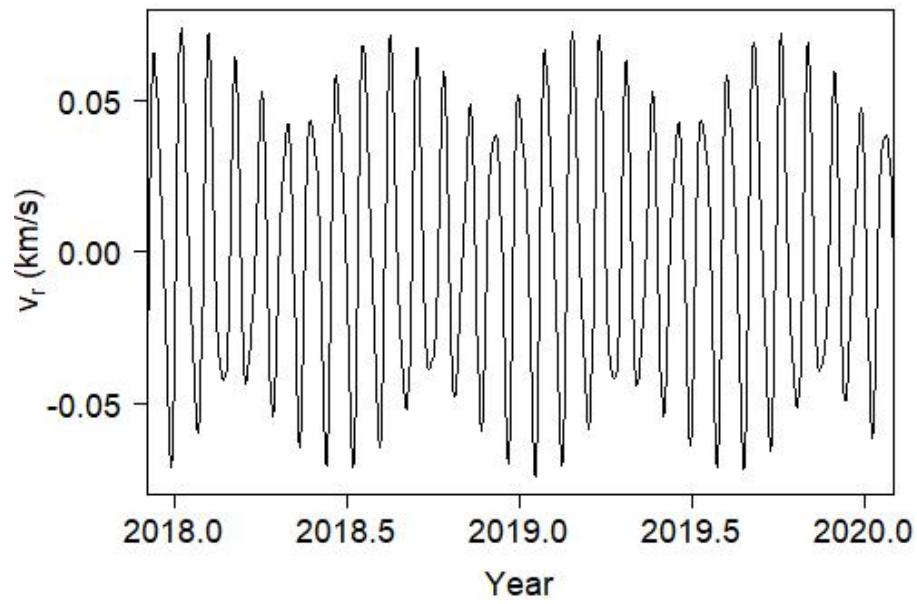


Figure 5: Radial velocity of the Moon relative to Earth from 2018 to 2020.

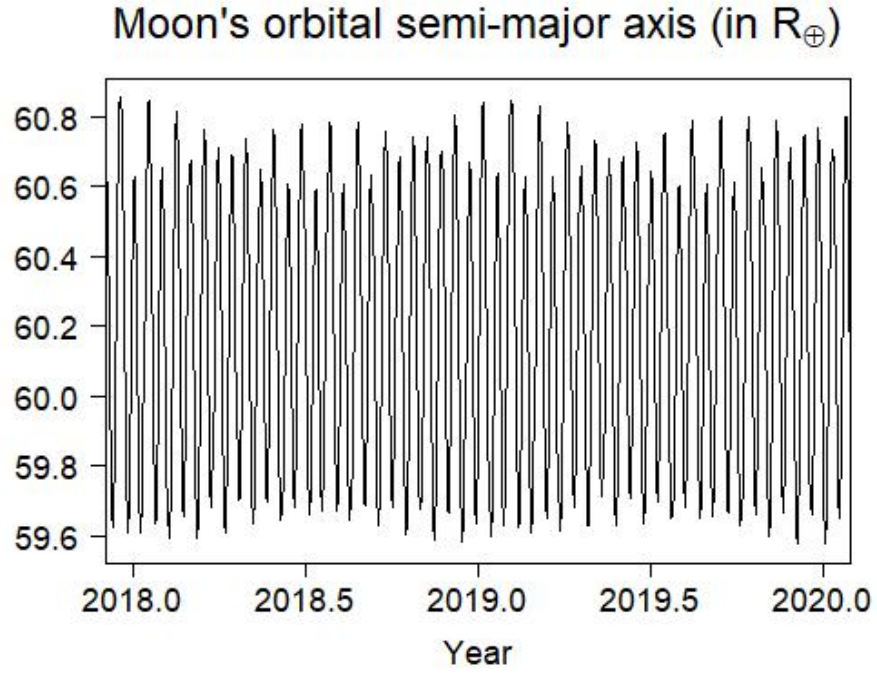


Figure 6: Orbital semi-major axis of the Moon from 2018 to 2020. Earth's radius is $R_{\oplus} = 6371$ km.

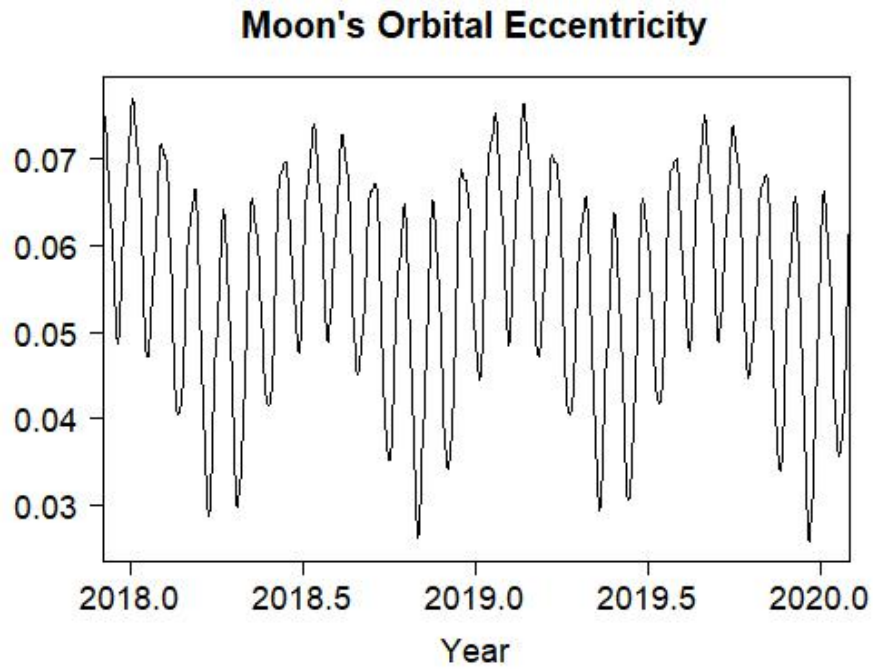


Figure 7: Orbital eccentricity of the Moon from 2018 to 2020.